BRANZ

OUT-OF-PLANE TESTING OF UNREINFORCED BRICK INFILL WALLS WITHIN STRUCTURAL FRAMES

AUCKLAND CBD, ORAKEI, HASTINGS, AND WELLINGTON, NEW ZEALAND

Final Report – LR0441

Submitted to BRANZ 30 June 2014

Jason Ingham, Kevin Walsh, Dmytro Dizhur, and Jalil Shafaei

j.ingham@auckland.ac.nz

Executive Summary

This report represents the final submission to BRANZ regarding research project LR0441.

Extensive research has been performed previously on modelling the out-of-plane (OOP) performance of unreinforced masonry (URM) walls and retrofitting URM load-bearing and infill walls for out-of-plane capacity. However, little empirical research has been performed within New Zealand on the seismically-induced behaviour of clay brick masonry infill walls within moment-resisting frames despite their prominence in the commercial building population. Hence, further research was proposed and pursued with an emphasis on testing URM infill walls (and retrofitting those infill walls that had cavities) based on an empirical testing approach wherein walls were loaded OOP using inflatable air bags. 21 separate tests were performed on 19 URM infill walls in four separate buildings.

Significant results that can be drawn from this research program are as follows:

◗ Restraint at the walls' vertical edges (horizontal boundaries), resulting in two-way OOP flexure as compared to one-way vertical OOP flexure, can substantially improve the OOP load-carrying capacity of tested infill walls;

◗ Topside fixed restraint and presumed "arching" action from the building frame can greatly increase the out-of-plane capacity of infill walls;

◗ In-plane damage can significantly reduce the out-of-plane capacity of a URM infill wall;

◗ Retrofit ties with adequate spacing and shear stiffness can greatly improve the out-of-plane capacity of URM cavity walls;

◗ The relative behaviour of the cavity walls tested in vertical flexure as well as visual observation of the failure mechanisms led the researchers to conclude that, if cavity tie spacing was held constant, then cavity tie diameter was the most important difference in the relative performance of the retrofitted cavity walls (as opposed to differences in model or installation mechanism);

◗ Increasing too greatly the OOP stiffness and strength of a wall spanning between rigid concrete elements can reduce its ultimate displacement capacity; and

◗ Material strengths related to brick compression, mortar compression, masonry bed joint shear, cavity tie pull-out, as well as other properties have been determined for a range of buildings in this typology.

Further testing and modelling of infill walls subjected to OOP loads are expected to be pursued in an effort to help translate the findings from this empirical study into specific recommendations in engineering standards and guidelines.

Contents

LIST OF FIGURES

LIST OF TABLES

1. Introduction and Scope

The earthquake vulnerability of buildings constructed using conventional British architecture and unreinforced masonry (URM) construction prior to the introduction of modern seismic loading standards is well-known in New Zealand based on observations from historical earthquakes. A high proportion of such structures in existence have not been strengthened to resist seismic forces. The performance of seismically deficient buildings (particularly of clay-fired brick URM construction) during the 2010-2011 Canterbury earthquakes was the most recent example of the vulnerability of URM construction when subjected to seismic lateral loads (Dizhur et. al. 2010, 2011; Ingham and Griffith 2011a, 2011b).

As a result of concern for the vulnerability of URM construction to earthquake loading, extensive research has been performed previously on modelling the out-of-plane (OOP) performance of URM load-bearing walls (Vaculik 2012; Derakhshan et al. 2013a, 2014; Walsh et al. 2014a) and retrofitting URM walls for out-of-plane capacity (Dizhur 2013; Dizhur et al. 2014). However, little empirical research has been performed within New Zealand on testing clay brick masonry infill walls within reinforced concrete (RC) moment-resisting frames – especially those with cavities – despite their prominence in the commercial building population (Walsh et al. 2014b). As a result, the out-of-plane capacity of such walls is generally only briefly addressed in currently available seismic assessment guidelines (NZSEE 2006).

1.1 Test scope and objectives

In order to meet the demand from the New Zealand engineering community regarding knowledge of the out-of-plane behaviour of brick URM infill walls, researchers at the University of Auckland physically tested walls in four different buildings (see **Figure 1**) utilising an approach consistent with the testing procedures developed by Derakhshan et al. (2013b) and Dizhur (2013). Application of lateral loads using airbags to simulate out-of-plane wall loads was used to accurately determine the out-of-plane capacity of internal URM partition walls and infill walls.

The objectives of the out-of-plane airbag testing performed on the walls within the four buildings and the associated results presented herein are expected to provide a basis of knowledge of the following characteristics:

◗ The OOP behaviour of clay brick infill walls in one-way "vertical" flexure as well as in two-way flexure;

◗ The effects of in-plane shear damage on the OOP initial stiffness and ultimate strength of infill walls;

◗ The OOP displacements that can be expected in infill walls prior to loss in strength and prior to collapse;

◗ Which cavity ties and cavity ties spacings are most effective in strengthening cavity walls and preventing OOP wall collapse;

◗ The pull-out strength of a variety of cavity ties; and

◗ Material strength of the in situ brick and mortar of infill walls in New Zealand.

The expected outcomes from this research program specifically involve three major "Industry Research Strategy Areas" from the *Building Research Association of New Zealand* (BRANZ):

◗ Materials performance – In addition to the mortar bed joint shear tests performed on site, samples of brick, mortar, and brick/mortar groups were taken to the University of Auckland's materials laboratory for compression and bond strength testing;

◗ Maintaining and improving the performance of existing buildings – RC frames with clay brick infill walls represent a prominent construction type from the 1920s - 1960s in New Zealand, and these

1

buildings are still in use for office, retail, industrial, and community services throughout the country; and

◗ Sustainability – Providing tools for precise assessment and efficient seismic retrofitting of these infill walls will reduce the energy, waste, and resources associated with new construction, partial reconstruction [e.g., replacement of bricks with reinforced concrete masonry units (CMU)], or retrofit solutions that are relatively costly and invasive (e.g., steel-framed backing).

Figure 1: Location of the four test buildings in the North Island of New Zealand and assumed years of original construction

1.2 Descriptions of buildings and associated test walls

1.2.1 Wellington Railway Station

The Wellington Railway Station building (hereafter referred to as the WRS building) is located on the north side of the Wellington CBD bordered by Thorndon Quay to the West, Bunny Street to the South, and Waterloo Quay to the East (see **Figure 2**). The WRS building was officially opened in 1937, although the exact year of construction of the components tested was not determined. The building is registered as a Category 1 Historic Place on the New Zealand Historic Places Trust Register (NZHPT 2014). Allegedly, the WRS building was the first major New Zealand structure to incorporate a significant measure of earthquake resistance (NZHPT 2014; IPENZ 2014). The building is a U-shaped structure

2

with the largest wing approximately 105 m long and 23 m high. The main building structure consists of five and six-storey steel-framed construction on top of the reinforced concrete piles. The steel structure is encased in reinforced concrete and clay bricks.

(a) Front elevation of the building

(b) Rear elevation of the building
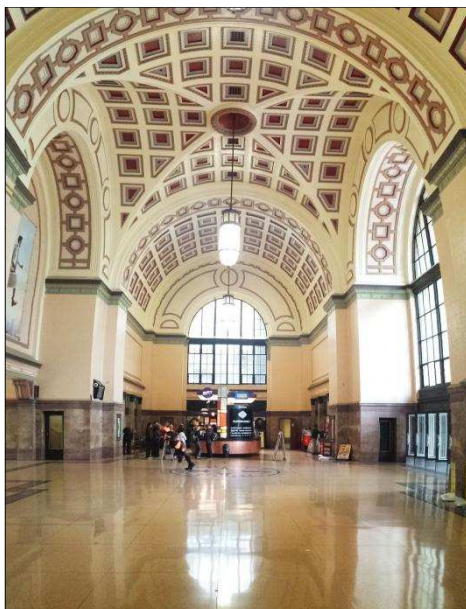
(c) Interior view of the main hall
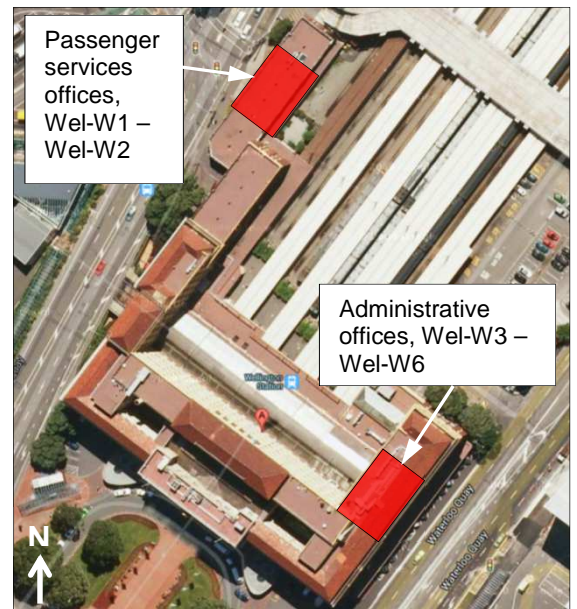
(d) Aerial image of the building and location of test walls

Figure 2: Elevations and aerial overview of the test wall locations at the Wellington Railway Station (WRS) building

The clay bricks used for the exterior cladding are slotted to accommodate vertical steel rods to reinforce the brickwork. Hence, the six walls that were tested in the WRS building (the test wall hereafter being denoted as Wel-W1 through Wel-W6) were all single-leaf, interior partition walls. One wall – Wel-W2 – was tested twice so as to determine its behaviour in both two-way and one-way flexure. The WRS test walls are shown in **Figure 3.**

Gypsum wall lining, moulding, piping, and air conditioning units were removed wherever possible from the test walls prior to testing. Vertical saw cuts were utilised in test walls Wel-W1, Wel-W2B, Wel-W3, Wel-W4, and Wel-W6 such that these walls behaved in one-way flexure only during applied loading. The single URM masonry leaf in these walls was wet cut using a concrete saw and where access was difficult, a dry cutting masonry saw was used as shown in **Figure 4**. Test wall Wel-W2A was tested with in situ boundary conditions in two-way flexure between a thickened brick pier and a return wall. Test wall

3

Wel-W5 was also tested with in situ boundary conditions in two-way flexure, although door openings also existed on both sides near return walls.

Wel-W1

(a) Loaded side of Wel-W1 with vertical saw cuts

(b) Instrument side of Wel-W1 with gypsum board intact

(c) Instrument side of Wel-W1 with gypsum board removed

Wel-W2

(d) Instrumented side of Wel-W2 with gypsum board intact

Wel-W3

(e) Instrumented side of Wel-W2 above the suspended ceiling level showing RC beam resting on brick pier

(f) Loaded side of Wel-W3 prior to test preparation

(g) Instrumented side of Wel-W3 prior to test preparation

Wel-W4

(h) Loaded side of Wel-W4 prior to test preparation

(i) Instrumented side of Wel-W4 prior to test preparation

Wel-W5

(j) Loaded side of Wel-W5 after gypsum board removal

Wel-W6

(k) Instrumented side of Wel-W5 prior to test preparation

(l) Loaded side of Wel-W6 after gypsum board removal and vertical saw cuts made

(m) Instrumented side of Wel-W6 after gypsum board removal and vertical saw cuts made

Figure 3: Test walls Wel-W1 – Wel-W6 at the Wellington Railway Station (WRS)
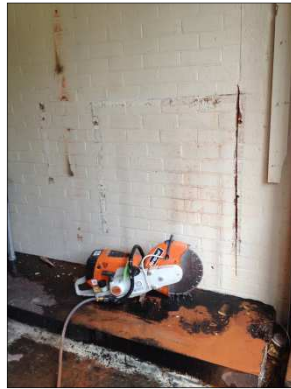
| (a) Wet saw used to create vertical cuts through the wall | (b) Dry saw used to extend vertical cuts through wall and extract bricks for bed joint shear testing |

Figure 4: Saw cuts during wall preparation for one-way vertical flexure

1.2.2 Orakei retail shops

The subject building located in Orakei, Auckland (see **Figure 5**) was originally constructed in 1938. At the time of the wall testing, the subject building was used as a multi-tenancy commercial building including retail and office space. The original construction plans for the building are incomplete and poor in legibility. Since its original construction, the building structure has remained mostly unchanged.

The subject building was constructed on a site sloping towards the southeast and features a partially buried basement level. As a result, the building is three storeys above grade along the northeast elevation and two storeys above grade along the southwest elevation. Overall, the building is rectangular-shaped in plan with no significant irregularities to its structure. The full height of the building is approximately 10 m to the top of the parapet along the northeast elevation.

The main structural system of the subject building consists of regularly spaced RC frames in the basement, ground and first floors and cavity (i.e., with an air gap between brick leaves) URM infill walls between the RC frames. The floor diaphragms consist of RC slabs in the ground and first floors and a suspended timber floor in parts of the basement level.

(a) Southwest elevation of the building

(b) Northeast elevation of the building and location of test walls

Ora-W1, exterior, two-leaf with cavity   Ora-W2, interior, single-leaf

Figure 5 continues on the following page

| (c) Interior view of the room with test walls | (d) Aerial image of the building and location of test walls |

Figure 5: Elevations and aerial overview of the test wall locations at the Orakei building

Two walls were tested out-of-plane at the Orakei building, as shown in **Figure 5** and **Figure 6**. A smooth lead damp-proof course extends through the entire thickness of the exterior brick leaf in the exterior cavity infill wall (Ora-W1) but only approximately 10 – 20 mm into the thickness of the interior leaf. Hence, a horizontal saw cut was made through the full mortar thickness of the interior leaf of Ora-W1 beneath the bottom brick course and the RC beam in order to simulate the bottom restraint condition assumed to be present on the accompanying exterior leaf due to the lead damp-proof course (i.e., laterally free). A horizontal saw cut was made through approximately half of the mortar thickness (i.e., 50 mm) of the lowest accessible brick course of Ora-W2, also to simulate the lead damp-proof course on the exterior wall (in order to create a conservatively representative set of testing conditions). Hence, the test walls heights noted in **Section 2.1** represent the height of the respective test wall from the horizontal saw cut to the underside of the top restraint.

Ora-W1

| (a) Tested side of Ora-W1 prior to the removal of appurtenances | (b) Tested side of Ora-W1 after the removal of appurtenances | (c) Exterior cavity wall with brick removed exposing the lead damp-proof course and air gap cavity |

Ora-W2

| (d) Tested side of Ora-W2 after the removal of appurtenances | (e) Side of Ora-W2 instrumented with digital callipers only |

Figure 6: Test walls W1 and W2 on the basement floor of the Orakei building

6

Twisted wire ties were also determined to be present in the exterior cavity wall (Ora-W1) and in good condition based on limited invasive inspection. However, the in situ tie spacing was not able to be determined. Typical cavity wall dimensions and in situ tie types with spacing for similar construction in New Zealand are described in Tasligedik et al. (2011).

1.2.3   Hastings offices and retail shops

The building tested in Hastings is located at 409-429 Heretaunga Street West. The original part of the building containing the test walls and housing retail space was constructed between 1931 and 1950 (assumed 1940s) as a moment-resisting RC frame with clay brick infill walls (see **Figure 7**). An annex to the east of the building currently housing offices was constructed between 1951 and 1975. Two leaves of clay brick masonry separated by a cavity serve as infill within the frame bays. The bricks serving as the frame infill are typically 74 mm deep x 112.5 mm thick x 240 mm long with 10 – 15 mm deep cement mortar joints. In situ twisted wire cavity ties were generally located at 900 mm horizontal spacing and 320 mm vertical spacing in a staggered fashion.

(a) Aerial image of the building and location test walls Has-W1 – Has-W6

(b) Exterior elevation of test walls Has-W1 – Has-W6 (left to right) after saw cutting

(c) Interior elevation of test walls Has-W1 – Has-W6 (right to left) after saw cutting

Figure 7: Elevations and aerial overview of the test wall locations at the Hastings building

Preparation of all walls in the Hastings building was performed by cutting through both leaves of the wall at such spacing as to produce six 1200 mm wide by 3750 mm tall sections of two-leaf masonry cavity walls separated from one another by approximately 50 mm and with in situ cavity reinforcing ties intact. All walls were tested with in situ ties left in place. Test wall Has-W5 was tested with only in situ ties, while all other test walls were retrofitted with 12 mm diameter by 230 mm long mechanical ties at different vertical spacings (see **Figure 8** and **Figure 9**). The top few rows of bricks were removed in test walls Has-W3 and Has-W4 and replaced with a timber support restraining horizontal translation while permitting rotation. This arrangement of boundary conditions more closely approximates URM partition walls that extend into timber-framed roofs (such as those on the fourth floor of the WRS building). All other walls were tested with the tops of the walls in their in situ condition, fixed by the RC beam above (see **Figure 10**).

(a) Pre-drilling cavity tie holes   (b) Installing mechanical ties   (c) Mechanical tie spanning cavity

Figure 8: Installing procedure for cavity restraint ties

Figure 9: Dimensions of test walls at the Hastings building and spacing of mechanical cavity ties

(a) Cross-section arrangement of test walls Has-W1, Has-W2, and Has-W6

(b) Cross-section arrangement of test walls Has-W3 and Has-W4

(c) Cross-section arrangement of test wall Has-W5
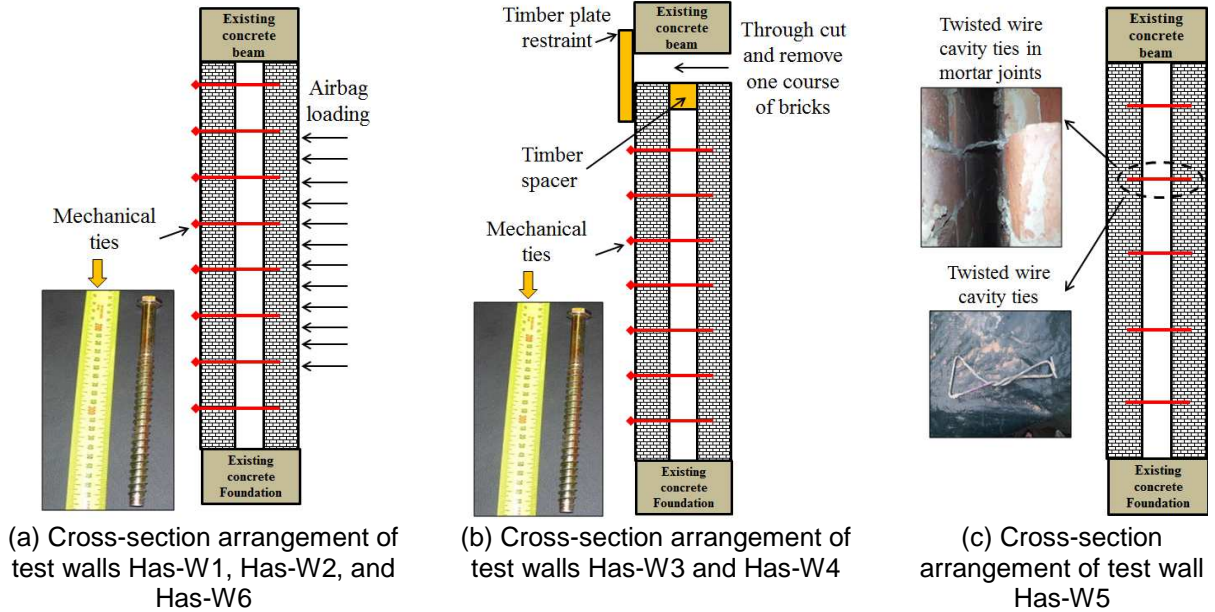
Figure 10: Test wall preparation of walls in the Hastings building in one-way flexure

1.2.4   Auckland CBD automobile mechanics shop

The test building was located on the lot at 151-165 Victoria Street West in the Auckland Central Business District (CBD) prior to its demolition for purposes of site redevelopment. The components of this building that were tested were originally constructed in 1958. The primary lateral load resisting system was comprised of a concrete-encased steel moment-resisting frame. On the exterior north and west walls that were tested in this program, two leaves of clay hollow-core brick with a cavity served as infill within the frame bays [see **Figure 11** and **Figure 12(a)**].

(a) Ariel image of the Hastings building and location of north and west testing walls
Figure 11 continues on the following page

(b) Interior of north wall prior to testing with test walls labelled and dimensions (in mm) shown

(c) Interior of west wall prior to testing with test walls labelled and dimensions (in mm) shown

Figure 11: Elevations and aerial overview of the test wall locations at the Auckland CBD building

In situ 4 mm diameter wire cavity ties twisted in a "figure eight" configuration were generally located at 900 mm horizontal spacing and 320 mm vertical spacing in a staggered fashion. The bricks were typically 73 mm deep x 107.5 mm thick x 227.5 mm long with 5 – 10 mm deep cement mortar joints. The frame and infill wall were connected by small concrete shear keys plus steel wires extruding from the RC columns into the mortar of the masonry walls (see **Figure 12**). At the base of the infill walls, there was a thin aluminium sheet placed between the mortar and concrete floor slab to prevent capillary water action. Typical cavity wall dimensions and in situ tie types and spacings for similar construction in New Zealand are described in Tasligedik et al. (2011).

(a) Cavity between two single-brick leaves of hollow-core bricks

(b) Twisted wire cavity ties in mortar joints

(c) Twisted "figure eight" wire cavity ties

(d) Concrete shear key and wire tie connection to the boundary column

Figure 12: In situ clay brick infill wall with cavity at the Auckland CBD building

10

Test walls Auc-W1, Auc-W2, and Auc-W3 were prepared by cutting through both leaves of the north wall at such spacing as to produce three 1200 mm wide x 3000 mm tall sections of two leaf masonry cavity walls separated by approximately 50 mm and with the in situ wire reinforcing ties intact. Auc-W1 was tested twice – initially with only the in situ ties and secondly with mechanical cavity ties added. Walls Auc-W2 and Auc-W3 were retrofitted prior to testing with chemical adhesive and alternative mechanical ties, respectively [see **Figure 13(a)**]. Auc-W4 and Auc-W5 were originally constructed as two-leaf infill masonry cavity walls, but the exterior leaf of each was removed prior to testing [see **Figure 13(b)**]. The single URM masonry leaf remaining in Auc-W5 was then cut diagonally in two planes with a circular saw to create a 50 mm deep step crack (in the shape of an "X" with the intersection of the cuts occurring near the centroid of the wall) in order to simulate a pre-existing in-plane crack from, hypothetically, a preceding earthquake [see **Figure 13(c)**].

| (a) The three retrofit ties used in addition to the in situ ties in Auc-W1B, Auc-W2, and Auc-W3, respectively (left to right) | (b) Removal of outer leaf for Auc-W4 and Auc-W5 | (c) Location of 50 mm deep simulated in-plane crack for Auc-W5 |
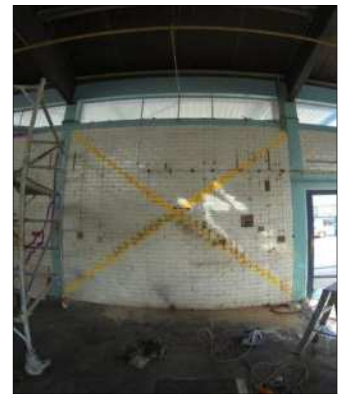
Figure 13: Test wall preparation at the Auckland CBD building

2. Experimental Program

2.1 Test walls

A total of 21 separate tests were performed on 19 distinct wall panels, as summarised in **Table 1**. The walls are ordered in **Table 1** primarily by the assumed year of building construction (as reported in the previous sections) and secondarily by the chronological order of walls tested in each building. Walls with a letter at the end of their designation represent the distinct wall panels that were tested in two different configurations each (e.g., Wel-W2A and Wel-W2B). All walls tested in one-way flexure were tested in "vertical" flexure such that the tops and bottoms were restrained in some fashion, and the sides of the walls were unrestrained. All walls tested in two-way flexure were restrained in some fashion on all four sides, with the exception of test walls Ora-W1 and Ora-W2, which were saw cut horizontally through the bottom edge to simulate the smooth lead damp-proof sheeting course present on the exterior leaf of the building.

Table 1: Summary of test wall geometry and cavity tie configuration

Test ID	# brick leaves	Flexure	Top edge restraint	Length (mm)	Test height (mm)	Cavity tie type	Tie diam./length (mm)	Tie spacing horiz./vert. (mm)
Wel-W1	1	One-way	RC slab	2180	4280	n/a	n/a	n/a
Wel-W2A	1	Two-way	RC slab	2662	4342	n/a	n/a	n/a
Wel-W2B	1	One-way	RC slab	1915	4342	n/a	n/a	n/a
Wel-W3	1	One-way	RC slab	3385	2700	n/a	n/a	n/a
Wel-W4	1	One-way	RC slab	1900	2450	n/a	n/a	n/a
Wel-W5	1	Two-way	Timber	2580	2980	n/a	n/a	n/a
Wel-W6	1	One-way	Timber	1305	2400	n/a	n/a	n/a
Ora-W1	2, cavity	Two-way*	RC slab	3346	2940	In situ	4 / "figure eight"	unknown
Ora-W2	1	Two-way*	RC beam	3380	2655	n/a	n/a	n/a
Has-W1	2, cavity	One-way	RC beam	1200	3950	Mechanical	12 / 230	600 / 338 (staggered)
Has-W2	2, cavity	One-way	RC beam	1200	3950	Mechanical	12 / 230	600 / 611
Has-W3	2, cavity	One-way	Timber	1200	3770	Mechanical	12 / 230	600 / 338
Has-W4	2, cavity	One-way	Timber	1200	3770	Mechanical	12 / 230	600 / 611
Has-W5	2, cavity	One-way	RC beam	1200	3950	In situ	4 / "figure eight"	900 / 320 (staggered)
Has-W6	2, cavity	One-way	RC beam	1200	3950	Mechanical	12 / 230	600 / 152
Auc-W1A	2, cavity	One-way	Timber	1200	2700	In situ	4 / "figure eight"	900 / 320 (staggered)
Auc-W1B	2, cavity	One-way	Timber	1200	2700	Mechanical	12 / 230	600 / 330
Auc-W2	2, cavity	One-way	Timber	1200	2700	Chemical	6 / 230	600 / 330
Auc-W3	2, cavity	One-way	Timber	1200	2700	Mechanical	8 / 220	600 / 330
Auc-W4	1	Two-way	Shallow RC beam	4400	3400	n/a	n/a	n/a
Auc-W5	1	Two-way	Shallow RC beam	4400	3400	n/a	n/a	n/a

* Bottom edge effectively unrestrained on Ora-W1 and Ora-W2 due to horizontal saw cut

The wall lengths listed in **Table 1** represent the distances between saw-cut edges for the walls tested in one-way flexure and the clear distance between presumably rigid horizontal boundary elements (e.g., columns, thickened brick piers, or return walls) for walls tested in two-way flexure. The test heights listed in **Table 1** represent the heights of the test wall panels between presumably rigid vertical boundary elements. In the case of a wall tested in one-way flexure, the test height represents the vertical length of the saw cuts, and that distance may be shorter than the vertical clear distance between the RC slab at the bottom of the wall and the RC slab, beam, or free end (the latter laterally secured by timber framing) at the top of the wall if the vertical saw cuts were not able to be made full-height. In the case of a wall tested in two-way flexure, the test height represents the clear distance between the rigid RC elements and/or the free ends.

2.2   Test setup and instrumentation

Loading was applied to all test walls by using an air compressor to gradually inflate one or two (depending on the length of the walls) vinyl airbags that were positioned in a gap of 25-35 mm between the test wall panel and a plywood backing. The plywood backing consisted of an assemblage of plywood sheets and timber frames [see **Figure 14(a) – (f)**]. The applied load from the airbags was transferred from the plywood backing to the braced reaction frame using six to eight s-shaped load cells (each with a capacity of 10 kN) which provided the primary source of horizontal stability to the plywood-backed frame panel. To ensure that the entire load was transferred through the load cells and not resisted by bearing friction, the plywood-backed frame panel rested on greased steel or Teflon^{TM} plates to allow the panel to slide with minimal frictional resistance [see **Figure 14(g)**]. The neighbouring braced reaction frame consisted of vertical and diagonal timber members screw fixed into the concrete floor slab. The total lateral load at any given time was calculated as the summation of the force recorded by all load cells.

| (a) Plywood backing frame being constructed | (b) Single vinyl airbag on plywood backing | (c) Reaction frame arranged to test two wall panels in sequence |
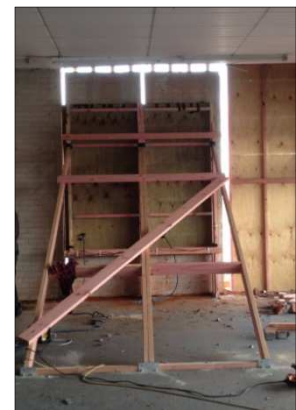
Figure 14 continues on the following page

(d) Reaction frame arranged to test one wall panel with two air bags inflated simultaneously
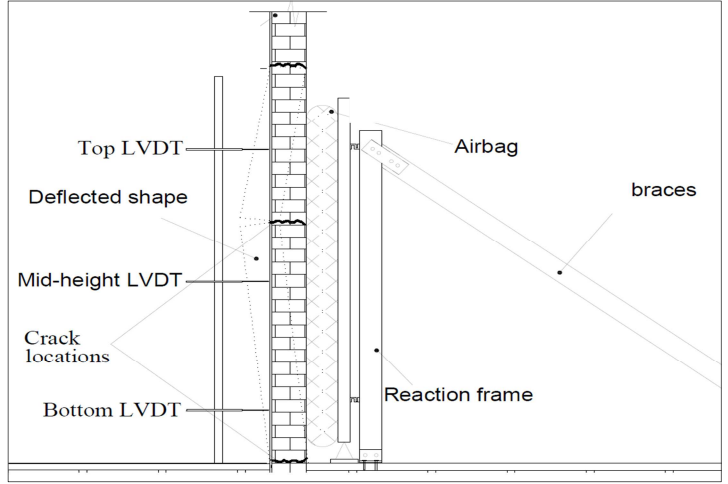
(e) Schematic of OOP test bracing (right of wall cross-section) and displacement instrumentation (left of wall cross-section)

(f) Profile of OOP test bracing (right of wall) and displacement instrumentation frame (left of wall)

(g) Close-up of base of reaction frame with s-shaped load cell placed between the plywood-backed panel frame and the braced reaction frame (top), and the plywood-backed frame sitting atop greased steel low-friction plates and loose plywood pieces

Figure 14: Components of braced reaction frame for OOP loading of test wall panels

The instrumentation used to measure the OOP displacement of each test wall was generally placed on an isolated frame located on the opposite side of the test wall to the loading frame [see **Figure 14(e)** and **(f)**]. The instrumentation frame supported as many as 15 strain gauges and three string potentiometers during any single test in this program [see **Figure 15(a) – (e)**]. Highly sensitive digital callipers were also placed redundant to other instrumentation at critical locations as a back-up and to provide comparative measurements [see **Figure 15(f)**]. A high-speed data acquisition (DAQ) system with multiple channels was used to record the test measurements at a frequency of at least 10 Hz [see **Figure 15(g)**]. The instrumentation layouts specific to individual walls are documented in the following sections.

14

(a) Displacement instrumentation frame for narrow-length wall

(b) Displacement instrumentation frame for medium-length wall

(c) Displacement instrumentation frame for long-wall with cracks from OOP two-way flexure highlighted

(d) Strain or "portal" gauge spanning between the test wall and the isolated instrumentation frame

(e) String potentiometer

(f) Redundant instruments (portal gauge, string potentiometer, and digital callipers) at the critical centre location on the test wall

(g) Data acquisition cable terminal (left) and computer (right)

Figure 15: Components of instrumentation for measuring OOP displacement of the test wall panels

2.2.1 Wellington Railway Station

Six distinct test walls were tested a total of seven times at the Wellington Railway Station. Examples of the test setup and instrumentation from the Wellington Railway Station are shown in **Figure 16**. The instrumentation layout is documented graphically in **Figure 17** (wherein G = strain gauge, S = string potentiometer, and L = load cell). Numerical values associated with the symbols used in **Figure 17** are included in **Table 2** and **Table 3**.

15

(a) Loaded side of Wel-W4 during testing

(b) Instrumented side of Wel-W5 during testing

(c) Loaded side of Wel-W6 during testing

Figure 16: Examples of the test setup and instrumentation at the WRS building

(a) Test wall cross-section showing loaded area and displacement gauges (reference **Table 2**)

(b) Test wall elevation showing the positions of the displacement gauges relative to the horizontal boundaries (reference **Table 3**)

Figure 17 continues on the following page

(c) Example of test wall elevation showing the positions of the load cells, loaded area and the position of the saw cuts (mm) for Wel-W1 and Wel-W2 only (Note: Dashed line indicates saw cut for Wel-W2B relative to load frame)

Figure 17: Test wall geometry and equipment layout at the WRS building
(Note: all measurements preceded by "≈" represent generic distances for purposes of simplicity)

Table 2: Summary of test wall vertical geometry and instrumentation at the WRS building [reference **Figure 17(a)**]

Test ID	Boundary and loading condition	h_{total} (mm)	h_{test} (mm)	$h_{load,1} =$ $h_{load,3}$ (mm)	$h_{cut,1}$ (mm)	$h_{cut,2}$ (mm)	h_1 (mm)	h_2 (mm)	h_3 (mm)	h_4 (mm)	h_5 (mm)	h_6 (mm)
Wel-W1	One-way flexure	4280	4280	1115	0	0	300	1127	713	713	987	440
Wel-W2A	Two-way flexure	4342	4342	1146	n/a	n/a	300	1147	724	724	n/a	1147
Wel-W2B	One-way flexure	4342	4342	1146	0	0	300	1147	724	724	n/a	1147
Wel-W3	One-way flexure	3100	2700	325	200	200	400	698	475	475	557	295
Wel-W4	One-way flexure	3100	2450	200	150	500	400	698	475	475	557	-5
Wel-W5	Two-way flexure	2980	2980	465	n/a	n/a	400	700	473	477	595	335
Wel-W6	One-way flexure	2980	2400	175	200	380	400	700	473	477	595	-45

Table 3: Summary of test wall horizontal geometry and instrumentation at the WRS building [reference **Figure 17(b)**]

Test ID	Boundary and loading condition	b_{total} (mm)	b_1 (mm)	b_2 (mm)	b_3 (mm)	b_4 (mm)	Horizontal length of air bag pressure zone (mm)
Wel-W1	One-way flexure	2180	90	1000	1000	90	2170
Wel-W2A	Two-way flexure	2660	270	605	605	1180	1900
Wel-W2B	One-way flexure	1915	230	605	605	475	1900
Wel-W3	One-way flexure	3385	200	1492	1493	200	2340
Wel-W4	One-way flexure	1900	200	750	750	200	1800
Wel-W5	Two-way flexure	2580	200	1090	1090	200	2340
Wel-W6	One-way flexure	1305	100	552	553	200	1170

2.2.2 Orakei retail shops

Two distinct walls were tested at the Orakei building. Unlike walls at any of the other buildings, OOP displacement of the tested walls at the Orakei building was measured using portal gauges and string potentiometers placed on the same side of the test walls as the reaction frame (due to restrictions on accessibility to the unloaded side of the test walls), but on separate, isolated frames so as to not be affected by deformations within the loading frame. Where the backside of test wall Ora-W2 was accessible for a short duration during testing, digital callipers were placed on a separate frame to supplement the measurements being taken by instrumentation on the loading side. Examples of the test setup and instrumentation from the Orakei building are shown in **Figure 18.** The instrumentation frame (placed on the same side of the test walls as the loading frame) supported as many as eight strain gauges and two string potentiometers simultaneously. The instrumentation layout is documented graphically in **Figure 19** (wherein G = strain gauge and S = string potentiometer). Values associated with the symbols used in **Figure 19** are included in **Table 4** and **Table 5**. The digital callipers placed on the opposite side of test wall Ora-W2 were located at approximately mid-height and mid-length of the wall (i.e., mirrored location relative to instrument S1).

| (a) Instrumentation framing on Ora-W1 (highlighted in blue) isolated from the reaction frame | (b) Test reaction frame at Ora-W2 | (c) Digital callipers placed on a separate frame against Ora-W2 |
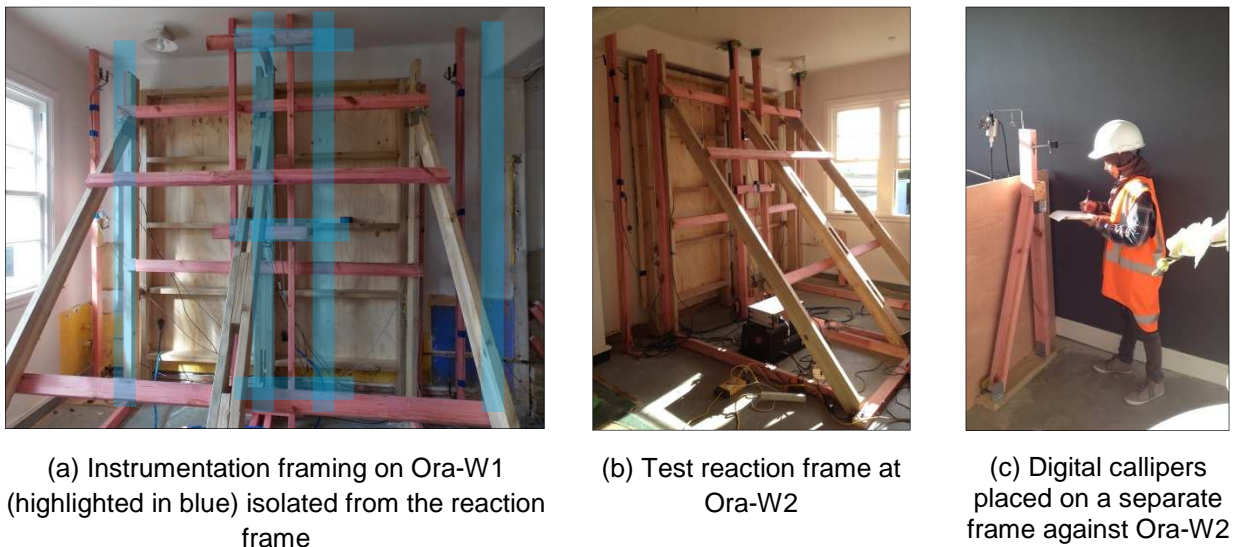
Figure 18: Examples of the test setup and instrumentation at the Orakei building

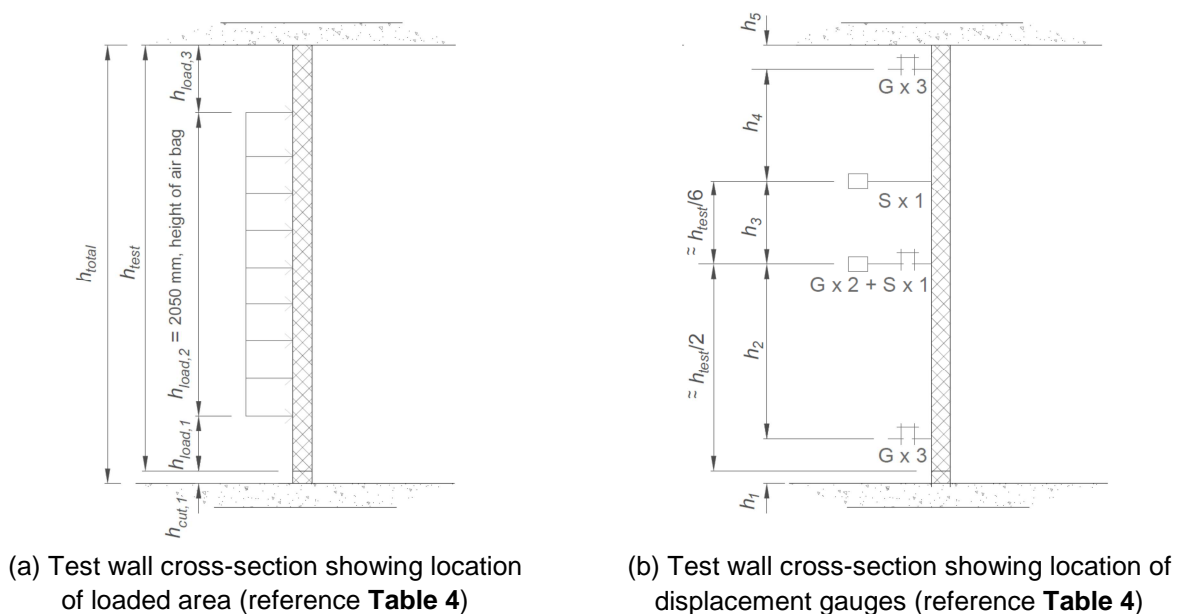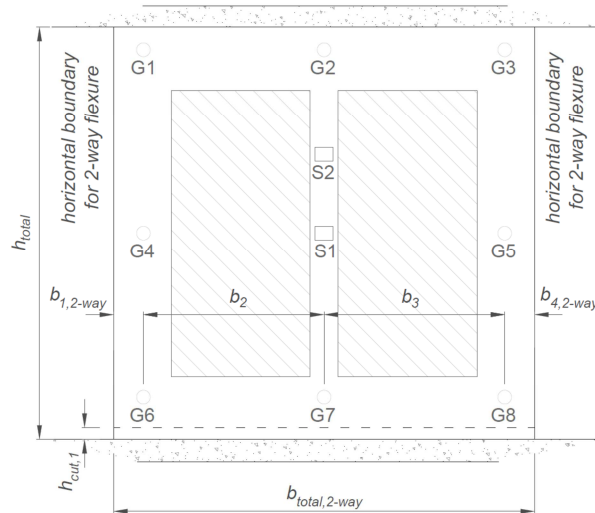| (a) Test wall cross-section showing location of loaded area (reference **Table 4**) | (b) Test wall cross-section showing location of displacement gauges (reference **Table 4**) |

Figure 19 continues on the following page

(c) Test wall elevation for W1 and W2 (reference **Table 4** and **Table 5**) [Note: dashed line indicates saw cut; hatched area indicates loaded area from airbags approximately 1150 x 2050 mm each]

Figure 19: Test wall geometry and equipment layout at the Orakei building
(Note: all measurements preceded by "≈" represent generic distances for purposes of simplicity)

Table 4: Summary of test wall vertical geometry and instrumentation at the Orakei building [reference **Figure 19(a) and (b)**]

Test ID	Boundary and loading condition	h_{total} (mm)	$h_{load,1}$ = $h_{load,3}$ (mm)	$h_{cut,1}$ (mm)	h_1 (mm)	h_2 (mm)	h_3 (mm)	h_4 (mm)	h_5 (mm)
W1	Two-way flexure & bottom edge free	2980	445	40	175	1335	490	845	135
W2		2725	302.5	70	133	1264 / 1376*	602 / 490*	663	63

* former value indicates distance to G4 and G5, and latter value indicates distance to S1

Table 5: Summary of test wall horizontal geometry and instrumentation at the Orakei building [reference **Figure 19(c)**]

Test ID	Boundary and loading condition	b_{total} (mm)	b_1 (mm)	b_2 (mm)	b_3 (mm)	b_4 (mm)	*Horizontal length of air bag pressure zone (mm)*
W1	Two-way flexure & bottom edge free	3436	259	1459	1459	259	2300 (total)
W2		3380	245	1445	1445	245	

2.2.3   Hastings offices and retail shops

Six distinct test wall panels (all cut from within the same larger wall panel) were tested at the Hastings building. The same, unaltered reaction frame and instrumentation frame were used for testing all of the walls in one-way flexure. Examples of the test setup and instrumentation from the Hastings building are shown in **Figure 20**. The instrumentation layout is documented graphically in **Figure 21** (wherein G = strain gauge and S = string potentiometer).

(a) Test reaction frame after testing Has-W1 to complete collapse and prior to testing Has-W2

(b) Instrumentation framing at Has-W1

(c) Lateral timber restraint anchored to the RC beam above Has-W3 and Has-W4

Figure 20: Examples of the test setup and instrumentation at the Hastings building
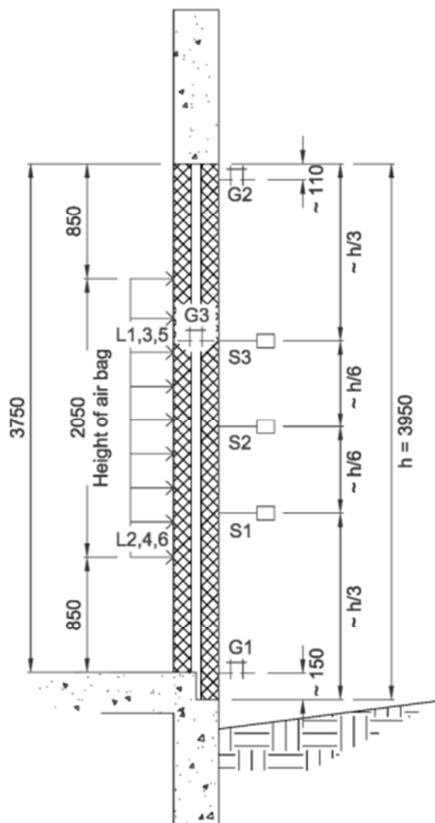
(a) Test wall cross-section showing location of displacement gauges for test walls Has-W1, Has-W2, Has-W5, and Has-W6
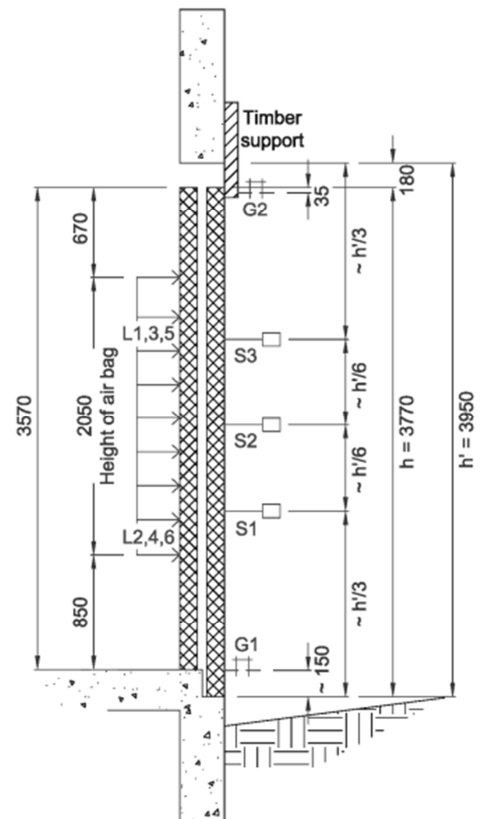
Test wall cross-section showing location of displacement gauges for test walls Has-W3 and Has-W4

Figure 21: Test wall cross-section showing location of loaded area and displacement gauges at the Hastings building

2.2.4   Auckland CBD automobile mechanics shop

Five distinct test wall panels (three cut from within the same larger wall panel) were tested a total of six times at the Auckland building. Examples of the test setup and instrumentation from the Auckland building are shown in **Figure 22**. Auc-W1, Auc-W2, and Auc-W3 were instrumented with a frame consisting of a single vertical post with two string pots located at 1500 mm and 2100 mm above the floor and a single steel portal gauge located 3000 mm above the floor. The same instrumentation frame was used for testing of all three one-way flexure walls. Auc-W4 and Auc-W5 required a much longer instrumentation frame [see **Figure 15(c)**]. The instrumentation frame for test walls Auc-W4 and Auc-W5 held in place twelve portal gauges and one string pot to measure the OOP displacement of the walls. The instrumentation layouts for all test walls in the Auckland building are documented graphically in **Figure 23** (wherein G = strain gauge, S = string potentiometer, and L = load cell).

| (a) Reaction frame set up to test Auc-W2 and Auc-W3 in one-way flexure in sequence | (b) Instrumentation framing at Auc-W3 in one-way flexure after Auc-W1 and Auc-W2 have been tested and cracked | (c) Reaction frame at Auc-W5 after testing caused partial OOP collapse of the wall in two-way flexure |

Figure 22: Examples of the test setup and instrumentation at the Auckland building
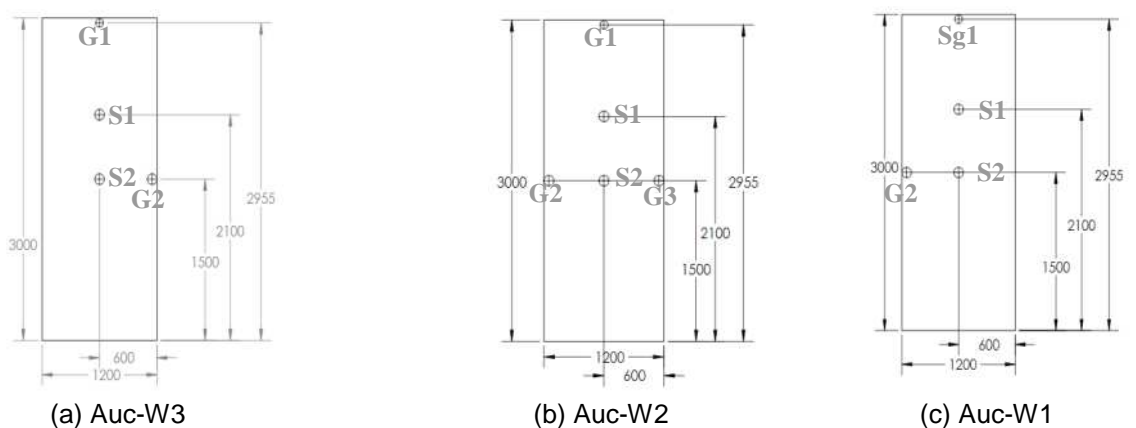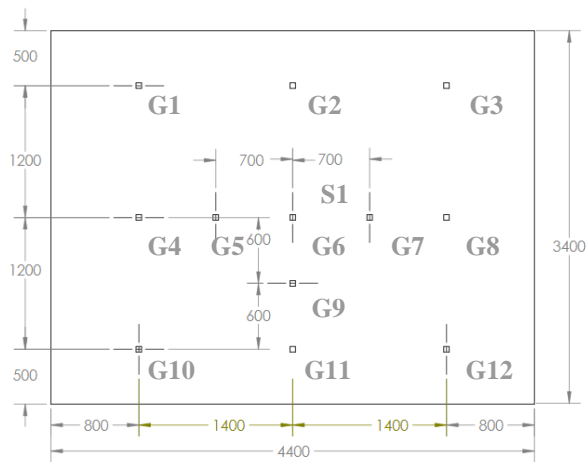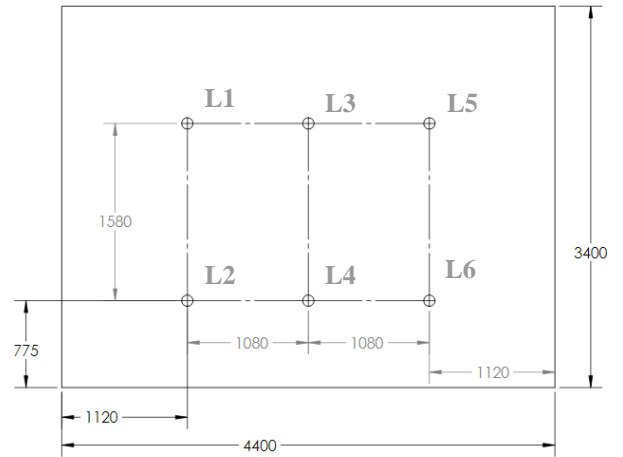

| (a) Auc-W3 | (b) Auc-W2 | (c) Auc-W1 |

Figure 23 continues on the following page

(d) Auc-W4 and Auc-W5 displacement instrumentation

(e) Auc-W4 and Auc-W5 load cell placement

Figure 23: Location of gauges at the Auckland building

3. Material strength characteristics

3.1 Masonry strength, stiffness, and density

Samples of brick and mortar were extracted from walls in all test buildings and taken to the University of Auckland materials laboratory for testing. Samples of brick and mortar were extracted from test walls Wel-W1, Wel-W2, Wel-W5, and Wel-W6 in the WRS building, were extracted from test wall Ora-W1 in the Orakei building, and were chosen randomly from the test walls in the Hastings and Auckland CBD buildings. (Note that different test walls were considered as having different densities in the WRS building per **Table 9** and **Table 12**.)

The compressive strength of mortar joint material was determined by compression testing of irregular mortar samples following the procedure reported by Valek and Veiga (2005). These irregular samples were extracted and cut into approximate cubical shapes having two parallel sides (i.e., top and bottom), capped using gypsum plaster, and tested in compression [see **Figure 24(a)** and **(b)**]. The mortar compression test results were then normalised following the procedures detailed in Lumantarna et al. (2014) to account for the irregular sample geometry. The extracted solid clay brick units were subjected to the laboratory half-brick compression test as shown in **Figure 24(c)** and **(d)**, consistent with the standard procedures of ASTM C67-11 (2011). Additional material test setups are illustrated in **Figure 24**.

(a) Typical mortar cube cut for testing prior to plaster capping

(b) Typical mortar compression test setup

(c) Typical clay brick cut into half-length and capped with plaster for compression testing

(d) Typical clay brick compression test setup

(e) Typical bond rupture test setup

(f) Bond rupture at interface of brick and mortar

Figure 24 continues on the following page

(g) Typical stacked masonry prism compression test setup with four portal gauges used to measure stiffness

(h) Typical brick rupture test setup

Figure 24: Examples of typical setups for testing extracted mortar and brick samples

A summary of the various material tests, relevant standards, and results is included in **Table 6**. Where appropriate samples for particular tests were not available, values were determined from empirically-based formulae (AIUMBER 2012; Almesfer et al. 2014). Characteristic "lower bound" material strength values may be derived by subtracting one standard deviation from the mean. Assuming that a normal distribution applies to the samples, 84% of the strengths for individual tested samples should be higher than these "lower bound" values, in this case. Note that the relative strengths of the bricks and mortar in the Hastings building are unusual, as most brick masonry in New Zealand is expected to be comprised of strong-brick/weak-mortar construction (Almesfer et al. 2014; Lumantarna et al. 2014).

Table 6: Summary of measured and calculated masonry material characteristics

Material characteristic	Associated standards and references for testing and processing results	Number of samples / **mean** / sample standard deviation (MPa unless noted otherwise)			
		Wellington Railway Station	**Orakei building**	**Hastings building**	**Auckland CBD building**
Mortar compression strength, f'_j	Valek and Veiga (2005), ASTM C1314-11a (2011) and Lumantarna et al. (2014)	23 / **12.8** / 3.7	6 / **8.4** / 3.4	8 / **27.9** / 7.2	5 / **13.9** / 1.2
Brick compression strength, f'_b	ASTM C67-11 (2011)	14 / **38.8** / 8.8	4 / **27.6** / 8.0	8 / **11.2** / 1.9	5 / **35.5** / 2.9
Stacked brick and mortar prism bond rupture strength, f'_{fb}	ASTM C1072-11 (2011)	**0.38**[*]	**0.25**[*]	4 / **0.28** / 0.10	**0.42**[*]
Stacked brick and mortar prism compression strength, f'_m	ASTM C1314-11a (2011)	**24.0**[*]	**16.3**[*]	3 / **8.2** / 1.6	2 / **9.4** / 2.8
Stacked brick and mortar prism elastic stiffness, E_m	ASTM C1314-11a (2011)	**7056**[*]	**4799**[*]	3 / **5356** / 1775	2 / **3504** / 1389
Brick rupture strength (modulus of rupture), f'_{mr}	ASTM C67-11 (2011)	**4.7**[*]	**3.3**[*]	**1.3**[*]	4 / **3.6** / 0.85
Stacked brick and mortar prism density, ρ_m (kg/m³)	ASTM C1314-11a (2011)	**1874**[*]	**1783**[*]	3 / **1659** / 15.9	3 / **1720** / 51.7

[*] Determined by equation (AIUMBER 2012, Almesfer et al. 2014)

3.2   Bed joint shear strength

In situ mortar bed joint shear tests were conducted in accordance with ASTM C1531-03, and the test setup is exemplified **Figure 25**. This type of test is moderately destructive as it requires the removal of at least one brick on one side of the test specimen to allow for insertion of a hydraulic jack, as well as the removal of a vertical mortar joint on the opposite side to allow horizontal bed joint movement to occur. The hydraulic jack was loaded using a pressure controlled hydraulic pump until visible bed joint sliding failure occurred. The bed joint shear strength was derived from the peak pressure records.

(a) Mortar bed joint shear test setup on Wel-W1

(b) Mortar bed joint shear test setup on Wel-W2 with cracks propagating from load highlighted in blue

(c) Mortar bed joint shear test setup on Auc-X1 (on otherwise untested wall)

(d) Mortar bed joint shear damage from testing on Auc-X1 (an otherwise untested wall) with shear cracks highlighted in red

Figure 25: Examples of typical mortar bed joint shear test setup

Masonry cohesion, c, is determined from individual shear strength test values (c_i) in accordance with the equation below (AIUMBER 2012):

$$c_i = \beta \left(\frac{V_H}{A_j} - Q_{G+Q} \right)$$

Where: V_H is the shear force at first movement of a masonry unit; A_j is the net mortared area of the bed joints above and below the test brick; Q_{G+Q} is the estimated gravity stress in the brick at the time of testing; and β is the collar joint reduction factor for multi-leaf masonry walls (β should be taken as 1.0 for single-leaf walls). The bed joint shear test results from this test program are summarised in **Table 7**.

Table 7: Summary of bed joint shear test results

Location	V_H (kN)	V_H/A_J (MPa)	β	σ_{G+Q}	c (MPa)	Failure type	Wall type
Wel-W1	90	1.8	1.0	0	1.8	No failure	Single leaf wall
Wel-W2	90	1.8	1.0	0	1.8	Vertical cracking through brick	Single leaf wall
Wel-W5	90	1.8	1.0	0	1.8	No failure	Single leaf wall
Wel-W6	42*	0.84	1.0	0	0.84	Vertical cracking through brick	Single leaf wall
Ora-W1	28	0.64	1.0	0	0.56	Brick sliding, failure in the mortar joints	Single leaf, part of two-leaf cavity wall
Ora-W1	25	0.60	1.0	0	0.52	Brick sliding, failure in the mortar joints	Single leaf, part of two-leaf cavity wall
Auc-X1	61	1.2	1.0	0	1.2	Cracking along bed joint top and bottom	Single leaf, part of two-leaf cavity wall
Aux-X1	75	1.5	1.0	0	1.5	Shear cracking in loaded brick	Single leaf, part of two-leaf cavity wall

* The bed joint shear capacity of Wel-W6 was likely artificially limited by the short length of the test wall

3.3   Cavity tie pull-out strength

The cavity ties used to retrofit test walls Auc-W1B, Auc-W2, and Auc-W3 were also tested in isolated pull-out tests, using the test set-up that is illustrated in **Figure 26.** The results are summarised in **Table 8**. Note that the 12 mm diameter mechanical tie type, which permitted test wall Auc-W1B to outperform its counterparts, also was found to have the highest isolated pull-out strength. However, cavity tie pull-out was not observed to limit the test wall capacities.

(a) Brace, load cell, and attachment used to pull out cavity tie from brick wall

(b) Pull-out failure due to brick conical shear

Figure 26: Pull-out test setup and example of failure mode in the Auckland CBD building

Table 8: Summary of pull-out testing results from the Auckland CBD building

| Cavity tie type	Tie diameter/length (mm)	Failure mode	Mean load capacity (kN)	Max load from single test (kN)
Mechanical	12 / 230	brick conical shear	15.16	27
Chemical	6 / 230	tie steel yield	8.66	9
Mechanical	8 / 220	pull out	1.82	2.5

4. Assessment considerations

4.1 Force-based assessment considerations

All tests walls listed in **Table 1** other than Ora-W1 and Ora-W2 rested on RC slab and were, therefore, presumed to be restrained laterally, axially, and rotationally along the bottom edge (i.e., restrained by a "fixed" support). Walls noted in **Table 1** as having a top edge restraint consisting of an RC slab or beam were also assumed to be restrained laterally, axially, and rotationally at the top edge as well (i.e., "fixed"). Walls noted in **Table 1** as having a top edge restraint consisting of timber were assumed to be restrained laterally but neither axially nor rotationally (i.e., restrained by a "propped" support). The shear and flexural implications of the two scenarios, at least in regard to "vertical" flexure, are illustrated in **Figure 27(a)** and **(b)**.

Many engineers in New Zealand will consider seismic demands on infill walls, whether derived from nonlinear time history analyses or simply from the loadings standard (NZS 1170.5:2004), based on OOP acceleration demands (i.e., force-based) in units of horizontal seismic acceleration (g). However, due to the test wall heights (i.e., saw cut heights often being short of the full heights of the in situ walls [$h_{test} < h_{total}$ per **Figure 27(c)** and **(f)**] and because the loading height is always short of the full height of the wall [$h_{load,2} < h_{total}$ per **Figure 27(c)** and **(f)**], the g-force values determined for walls in one-way vertical flexure must be converted to represent uniformly distributed earthquake loads over the full-height walls [see **Figure 27(e)** and **(h)**]. The results of this conversion from the test scenario to the assessment scenario for wall tested in one-way vertical flexure are summarised in **Section 5.1.4**. Note that the "pivot point" in the conversion from test wall to full-height wall is the maximum flexural capacity of each wall at a given cross-section. In other words, the test walls illustrated in the scenarios represented by **Figure 27(d)** and **(e), or Figure 27(g)** and **(h)**, are assumed to have the same flexural capacity at mid-height despite having different heights and loading distributions. For example, in the case of a wall with fixed-propped restraints [see **Figure 27(g)**], the flexural moment at the mid-height crack location when subjected to the maximum load is derived as follows:

$$M(\beta h_{test}) = \left(h_{load,2}w_{test} + \frac{\left(h_{load,2}w_{test}\left(h_{load,2}^{3} + 4h_{load,2}^{2}h_{load,3} + 6h_{load,2}h_{load,3}^{2} + 4h_{load,3}^{3} \right) \right) - \left(h_{load,2}h^{2}w_{test}\left(6h_{load,2} + 12h_{load,3} \right) \right)}{8h_{test}^{3}} \right)(1-\beta)h_{test}$$
$$- w_{test}\frac{\left((1-\beta)h_{test} - h_{load,3} \right)^{2}}{2}$$

This flexural capacity, $M(\beta h_{test})$, is then presumed to represent the mid-height flexural capacity in the full-height scenario [see **Figure 27(b)** and **(h)**], such that the effective uniformly distributed load, w_{eff}, can be derived. Note that all walls that were tested in a fixed-propped condition (in some cases, by removing the top few rows of bricks from beneath the RC beam above and introducing a timber restraint) were assessed as if their in situ condition was fixed-propped regardless of the actual in situ condition, such that the effect of the different restraint conditions could be considered. Such conversions of measured test capacities to effective full-height capacities were not performed for walls tested in two-way flexure. Because all walls tested in two-way flexure were tested in their full-height condition with loading concentrated near the centre of each wall, the horizontal seismic acceleration capacities (g) presented in **Section 5.2.4** are assumed to be slightly conservative.
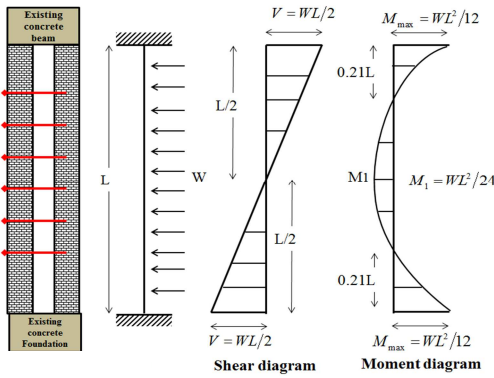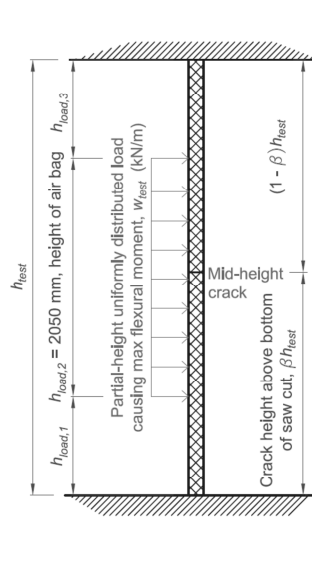
(a) Assumed shear and moment response of walls fixed at both the top and bottom
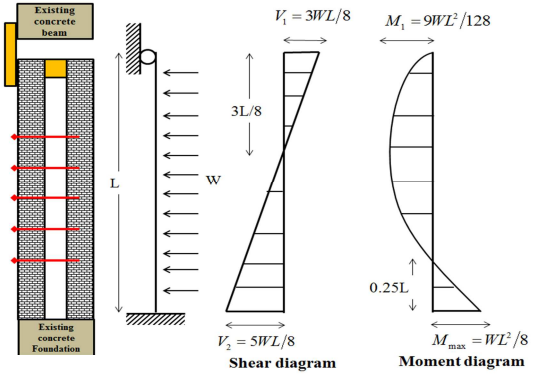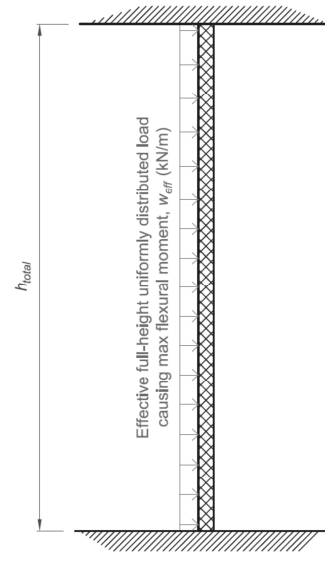
(b) Assumed shear and moment response of walls fixed at the bottom and propped at the top
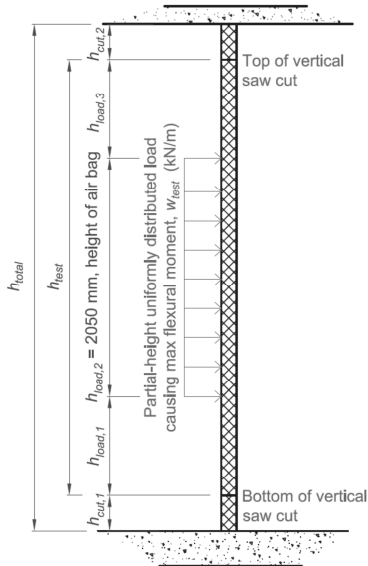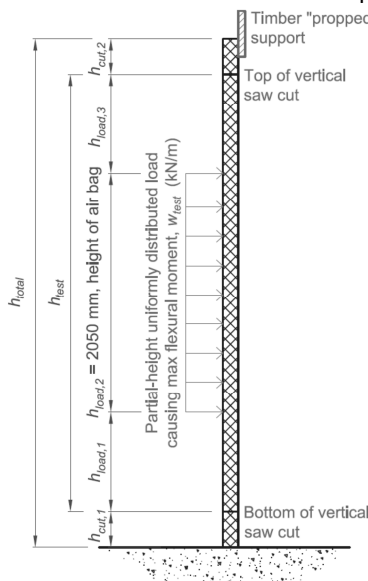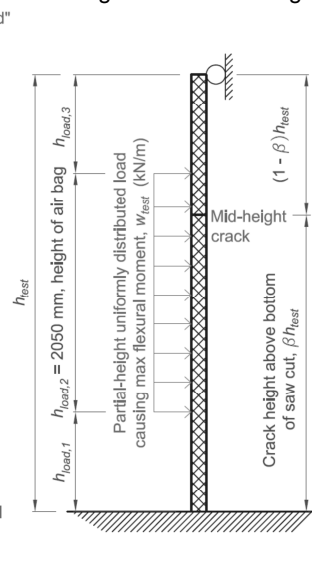
(c) Actual test condition for fixed-fixed wall

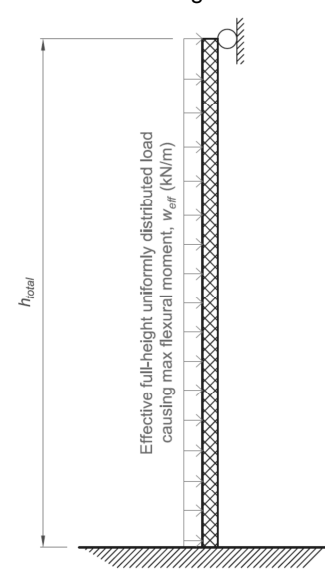(d) Assessed condition for fixed-fixed wall with test height and partial-height uniform loading

(e) Assessed "effective" condition for fixed-fixed wall with in situ full height and full-height uniform loading

(f) Actual test condition for fixed-propped wall

(g) Assessed condition for fixed-propped wall with test height and partial-height uniform loading

(h) Assessed "effective" condition for fixed-propped wall with in situ full height and full-height uniform loading

Figure 27: Cross-sections of test walls with different restraint conditions, associated wall behaviours, and assessment considerations for testing in one-way "vertical" flexure

28

4.2 Other assessment considerations

Assessing walls in one-way vertical flexure in regard to force-based capacity may be the most straightforward and conservative approach in consulting practise, but considering two-way flexure or displacement-based assessment techniques may provide more accurate or useful results. Recent research has incorporated these advanced considerations into modelling of the OOP performance of URM load-bearing walls (Griffith and Vaculik 2007; Vaculik 2012; Derakhshan et al. 2013a, 2014). Both models have boundary restraint conditions that can be adjusted to more appropriately simulate the behaviour of URM infill walls (as opposed to load-bearing walls) such as those tested in this research program. Note that one of the future objectives of this research program is to utilise the empirical data from URM infill testing to calibrate boundary restraint conditions appropriate to URM infill walls.

The procedure proposed by Derakhshan et al. (2013a) for the numerical assessment of URM walls subjected to OOP loading was used to develop the idealised displacement-load relationships for some walls tested in one-way vertical flexure as presented in **Section 5.1.2**. This procedure is largely based on the geometric attributes of URM walls. After developing mid-height horizontal cracks, vertical wall "strips" are assumed to deform through rocking mechanisms [see **Figure 28(a)**] and these mechanisms are sensitive to dynamic inputs, which are not addressed in the quasi-static loading protocol of this research program.

A virtual work-based, two-way flexural analysis, which includes weighted components of horizontal flexure (i.e., flexure about a vertical axis) and diagonal flexure [see **Figure 28(b)**], can be conducted by implementing the design procedure of AS 3700:2011 and Think Brick Australia (2013). In practise, walls may be assessed considering both vertical flexure and two-way flexure. The capacity limit state with the higher value between vertical flexure and two-way flexure may be presumed to govern for any specific wall panel given the inherent conservativeness in the idealised failure modes presumed by each method.

(a) Rocking mechanism of wall tested in one-way vertical flexure (Derakhshan et al. 2014)

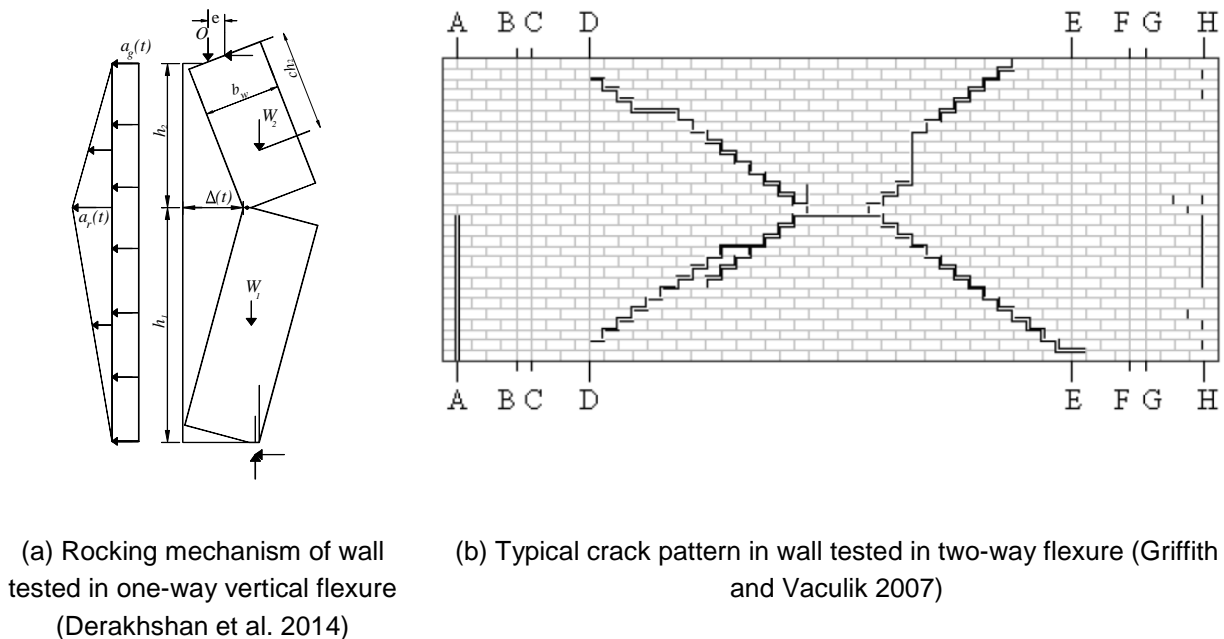(b) Typical crack pattern in wall tested in two-way flexure (Griffith and Vaculik 2007)

Figure 28: Typical damage mechanisms for URM walls subjected to OOP loading

5.   Test Results

5.1   Walls tested in one-way vertical flexure

Within the entire test program, 14 distinct test wall panels were tested a total of 15 times in one-way vertical flexure (with the remaining six tests being performed in two-way flexure). The geometries of those walls are summarised in **Table 9**. Note that the total thickness without ("w/o") including the cavity width represents the thickness of two bricks in the case of the two-leaf cavity walls and is considered in this fashion for purposes of determining wall weights. Except where indicated in **Table 9**, masonry density was based on dimensional measurements and weighting, as noted in **Section 3.1**.

Table 9: Summary of geometry of walls tested in one-way vertical flexure

| Test ID	# brick leaves	Top edge restraint condition	Length (mm)	Test height (mm)	Mean masonry density (kg/m^3)	Total thickness of wall w/o cavity (mm)	Total thickness of wall incl. cavity (mm)	Cavity tie
Wel-W1	1	Fixed	2180	4280	1837*	108	108	n/a
Wel-W2B	1	Fixed	1915	4342	1926*	108	108	n/a
Wel-W3	1	Fixed	3385	2700	1868*	108	108	n/a
Wel-W4	1	Fixed	1900	2450	1868*	108	108	n/a
Wel-W6	1	Unconf.	1305	2400	1853*	108	108	n/a
Has-W1	2, cavity	Fixed	1200	3950	1659	225	290	Mech.12 mm dia. @ 338 mm vert.
Has-W2	2, cavity	Fixed	1200	3950	1659	225	290	Mech.12 mm dia. @ 611 mm vert.
Has-W3	2, cavity	Unconf.	1200	3770	1659	225	290	Mech.12 mm dia. @ 338 mm vert.
Has-W4	2, cavity	Unconf.	1200	3770	1659	225	290	Mech.12 mm dia. @ 611 mm vert.
Has-W5	2, cavity	Fixed	1200	3950	1659	225	290	In situ
Has-W6	2, cavity	Fixed	1200	3950	1659	225	290	Mech.12 mm dia. @ 152 mm vert.
Auc-W1A	2, cavity	Unconf.	1200	2700	1720	215	268	In situ
Auc-W1B	2, cavity	Unconf.	1200	2700	1720	215	268	Mech.12 mm dia. @ 330 mm vert.
Auc-W2	2, cavity	Unconf.	1200	2700	1720	215	268	Chem. 6 mm dia. @ 300 mm vert.
Auc-W3	2, cavity	Unconf.	1200	2700	1720	215	268	Mech.8 mm dia. @ 330 mm vert.

* Stacked masonry prism elements (consisting of multiple bricks and mortar joints intact) were not able to be extracted from the WRS building. Hence, the density in this case was determined based on the brick and mortar compression strengths as explained in **Section 3.1**.

### 5.1.1   Load-displacement response of walls tested in one-way vertical flexure

All test walls were loaded semi-cyclically at a quasi-static loading rate. The left vertical axes in **Figure 29** represent the total test load (i.e., combination of loads measured by all of the individual load cells) divided by the weight of each wall, expressed as a result in terms of horizontal seismic acceleration (g). The wall geometries and masonry material densities used to determine the horizontal acceleration capacity of each wall are listed in **Table 6**. Note that the values of horizontal acceleration (g) shown in **Figure 29** are based on the test height (as described in **Section 2.1** and listed in **Table 6**) and the total test load as distributed over a partial height of the wall, and are therefore not necessarily representative of the effective horizontal acceleration capacity of the full-height wall subjected to uniformly distributed seismic loads, as addressed in **Section 5.1.4**. Where walls were able to be tested to complete collapse, the instability drift was measured using photogrammetry, and idealised load-displacement curves are included as derived from relationships published by Derakhshan et al. (2013a).
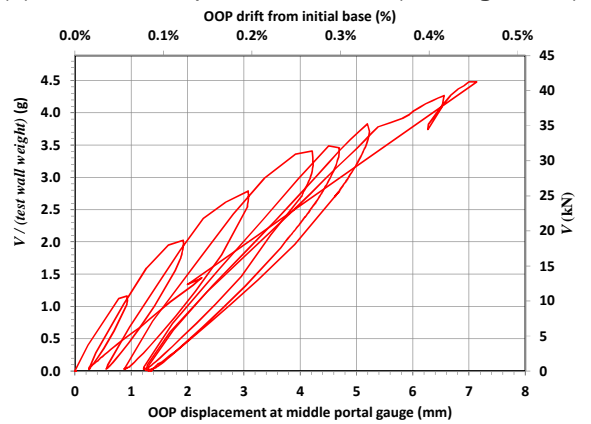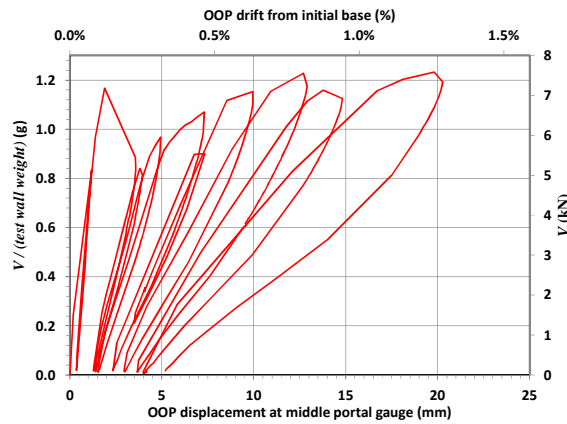
30
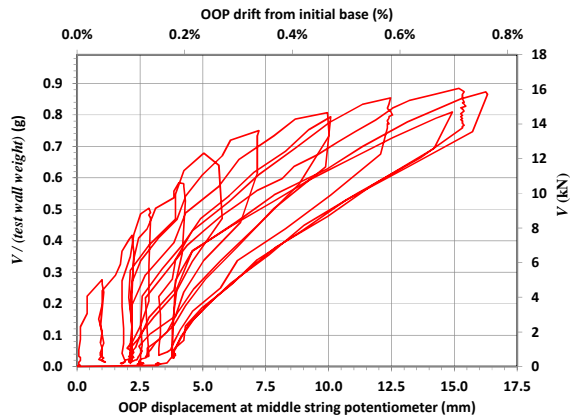
(a) Wel-W1 displacement at S2 (see **Figure 17**)
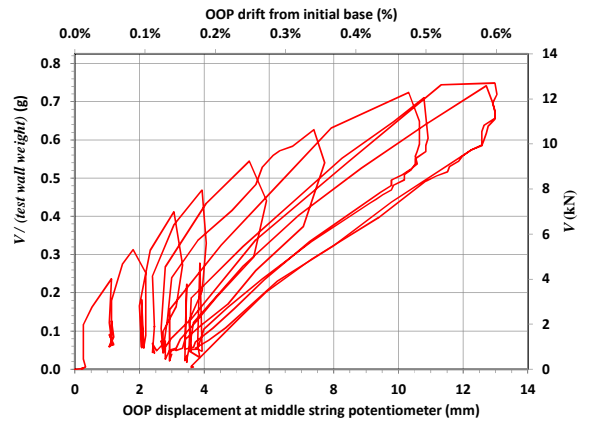
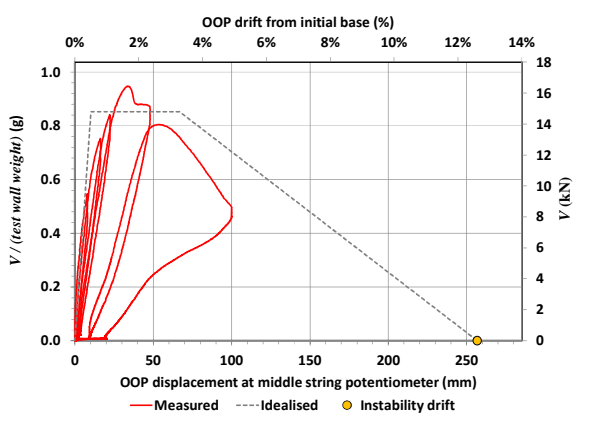(b) Wel-W2B displacement at S2 (see **Figure 17**)
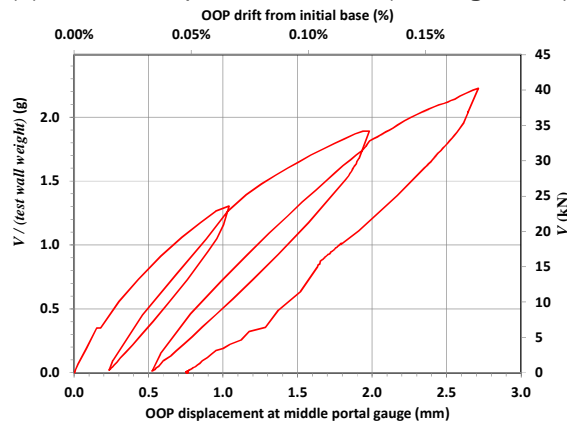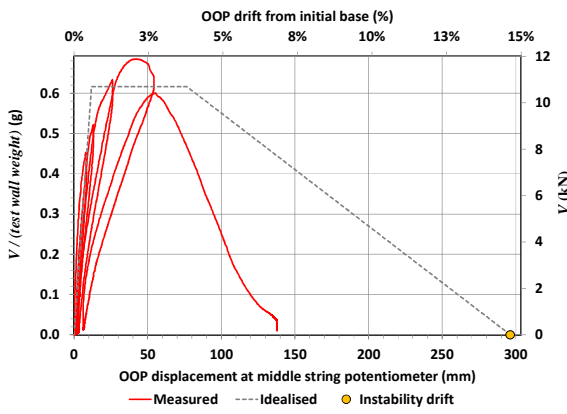
(c) Wel-W3 displacement at G8 (see **Figure 17**)

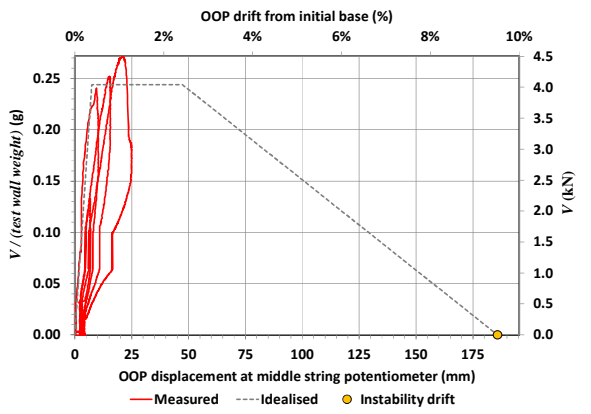(d) Wel-W4 displacement at G8 (see **Figure 17**)

(e) Wel-W6 displacement at G8 (see **Figure 17**)

(f) Has-W1 displacement at S2 (see **Figure 21**)

(g) Has-W2 displacement at S2 (see **Figure 21**)

(h) Has-W3 displacement at S2 (see **Figure 21**)

Figure 29 continues on the following page
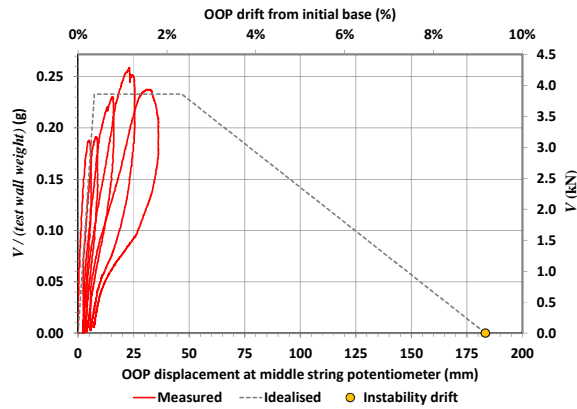
(i) Has-W4 displacement at S2 (see **Figure 21**)
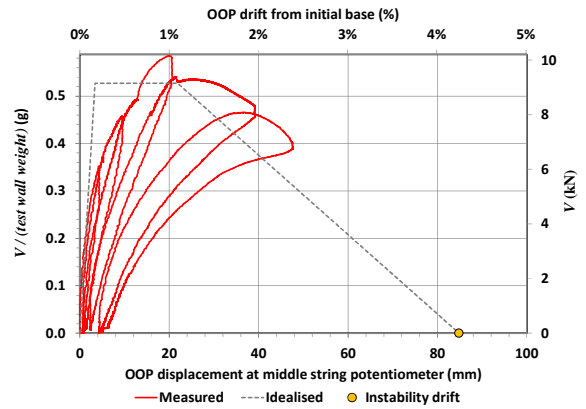
(j) Has-W5 displacement at S2 (see **Figure 21**)
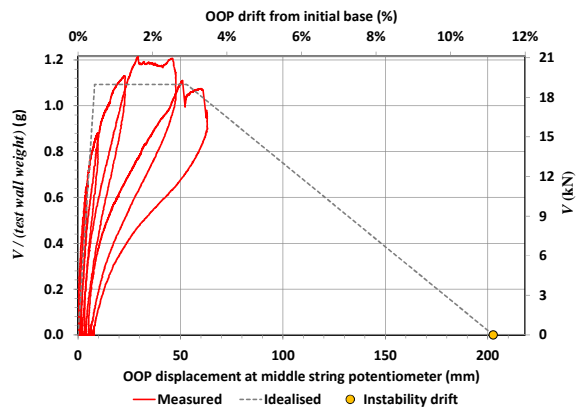
(k) Has-W6 displacement at S2 (see **Figure 21**)
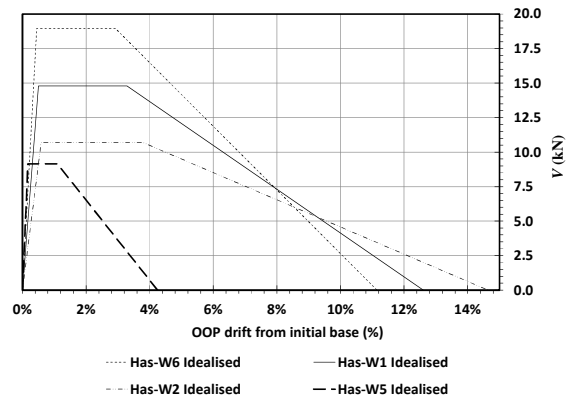
(l) Idealised responses of Hastings fixed walls
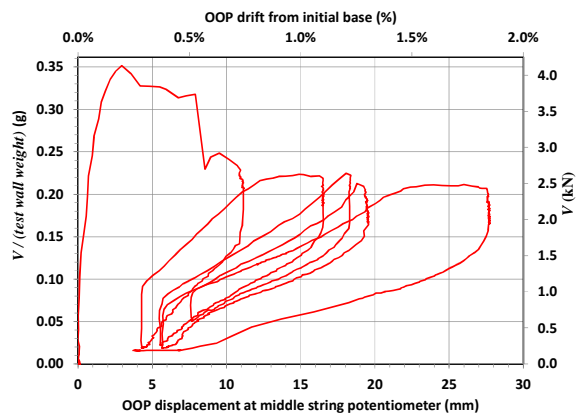
(m) Auc-W1A displacement at S2 (see **Figure 23**)

(n) Auc-W1B displacement at S2 (see **Figure 23**)

(o) Auc-W2 displacement at S2 (see **Figure 23**)

(p) Auc-W3 displacement at S2 (see **Figure 23**)
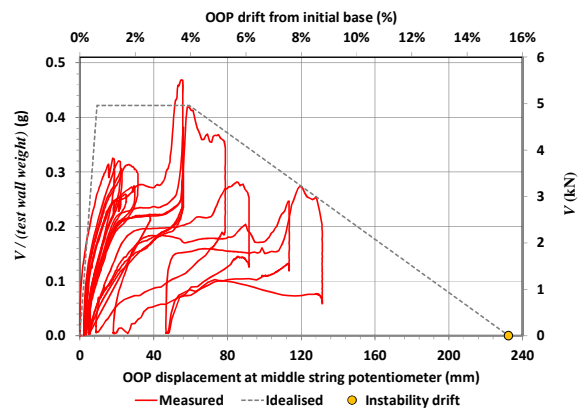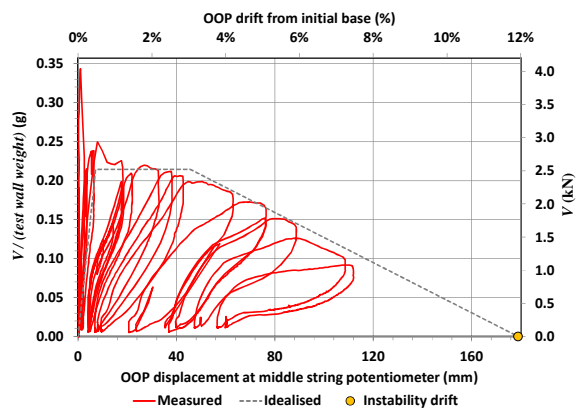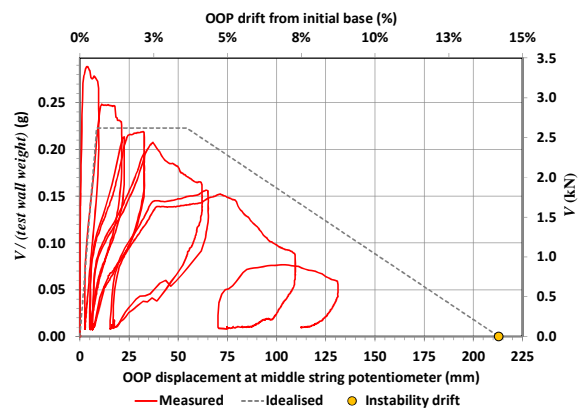
Figure 29: Load-displacement responses for walls tested in one-way vertical flexure

32

The following comments should be considered in conjunction with the force-displacement plots shown in **Figure 29**:

- The test walls at the WRS building needed to be reinstated after testing and so could not be loaded until collapse;

- Walls Wel-W1 and Wel-W2B were loaded until residual displacements and a plateau in load capacity were measured, as shown in **Figure 29(a)** and **(b)**;

- Walls Wel-W3 and Wel-W4 were each loaded until the capacity of the loading frame or load cell instrumentation was reached. The load-displacement curves in **Figure 29(c)** and **(d)** for walls Wel-W3 and Wel-W4, respectively, appear close to plateauing at the peak loads and are hence considered to finish just short of the peak load capacities of the test walls, although it should be noted that wall Wel-W3 was the only wall tested in vertical flexure in this entire program that was not successfully cracked near mid-height (nor was any other cracking apparent on Wel-W3);

- Wall Wel-W6 was loaded until the maximum load plateaued with increasing incremental displacements. The force-displacement profile in the early cycles shown in **Figure 29(e)** for the wall is likely to be influenced by the brick lintel that existed above the wall (due to the saw cut not being full height). As the test progressed beyond the initial cycles, the brick lintel cracked and lost its rigidity, leaving W6 effectively propped at the top edge in the later load cycles;

- The relative behaviour of test walls Has-W1 – Has-W6 as shown in **Figure 29(f)** – **(I)** led researchers to conclude the following:

  o Retrofit ties with adequate spacing and shear stiffness can greatly improve the out-of-plane capacity of URM cavity walls. For a force-based analysis, the wall strip strength was approximately doubled from the in situ condition to the condition in which ties were vertically spaced at approximately 150 mm considering the test walls with fixed topside restraints [compare the relative performance of in situ Has-W5 with retrofitted Has-W6 in **Figure 29(I)**]. An even greater improvement in displacement-based performance was observed;

  o Increasing a fixed wall's out-of-plane stiffness and strength too greatly can reduce its ultimate displacement capacity [compare the relative performance of Has-W6, Has-W1, and Has-W2, each with progressively larger cavity tie spacing, in **Figure 29(I)**]; and

  o In comparison to the results from the test walls in the Auckland CBD building [**Figure 29(m)** – **(p)**] as well as two other wall panels in Hastings that were propped on the top edge [**Figure 29(h)** and **(i)**], it is clear that top edge fixed restraint condition improves the load capacity of the wall panels significantly; and

- As in the rest of this report, the walls are listed in **Figure 29** in the order of original building construction. However, in the test program itself, the walls in the Auckland building were tested firstly. The relative behaviour of the cavity walls tested in vertical flexure at the Auckland CBD building as well as visual observation of the failure mechanisms led the researchers to conclude that, if cavity tie spacing was held constant, then cavity tie diameter was the most important difference in the relative performance of the retrofitted cavity walls (as opposed to differences in model or installation mechanism), which is logical given the relationship between cavity tie diameter and shear flow capacity. Adhesive cavity ties were not notably more useful to improving OOP cavity wall performance than were more easily inserted mechanical cavity ties. Hence, when the six walls in the Hastings building were tested in similar fashion, only the tie type used in test wall Auc-W1B was utilised (i.e., the mechanical cavity tie with a 12 mm diameter), and the variables considered in Hastings were vertical tie spacing and wall top fixity only.

5.1.2 Displacement profiles of walls tested in one-way vertical flexure

The horizontal and vertical maximum displacement profiles for all walls tested at the Wellington Railway Station in one-way vertical flexure are shown in **Figure 30**. (Note that displacement profiles are not provided for the walls tested in vertical flexure at the Hastings and Auckland CBD buildings due to those walls being measured with only one line of instrumentation and due to those particular test walls being loaded to their instability displacements, during which the displacement instrumentation was removed.) The New Zealand loadings standard for earthquake actions (NZS 1170.5:2004) requires that connections for "parts and components" of buildings (such as infill walls subjected to OOP demands) be designed and assessed for larger demands than the components themselves should sustain. If it is assumed that the mortar course between the reinforced concrete slab or beam and the masonry infill wall qualifies as the "connection" of these components for purposes of the standard, then the stiffness and capacity of this interface can begin to be understood by examining the displacements of each wall near the RC slabs or beams at top and bottom during loading (as well as from the results of bed joint shear tests addressed in **Section 3.2**).

The vertical displacement profiles in **Figure 30** all appear to trend toward zero displacement at the top and bottom of the walls, suggesting a high shear rigidity and capacity at these locations, especially considering the high shear demands at the fixed boundaries (see **Figure 27**). Note that some of the horizontal displacement profiles in **Figure 30** exhibit eccentric wall response. For example, **Figure 30(g)** and **(h)** chart the displacement profiles for test wall Wel-W4, and the eccentric response apparent in these charts is the result of a short return wall positioned on the left side of Wel-W4 (i.e., nearest portal gauge line G1,4,7,10,13).

Wall Wel-W6 was propped at the top by lightweight timber framing, as compared to test walls Wel-W1 – Wel-W4 which were fixed at the top by a RC slab. String potentiometers were placed on the topside of Wel-W6 and secured to the roof framing in order to measure the axial elongation on the "tension side" of the wall under one-way vertical flexure. The maximum vertical "uplift" as measured by one of the string potentiometers was 2.8 mm. Uplift displacement should be taken into consideration if a topside securing mechanism is designed and implemented for similarly propped walls.
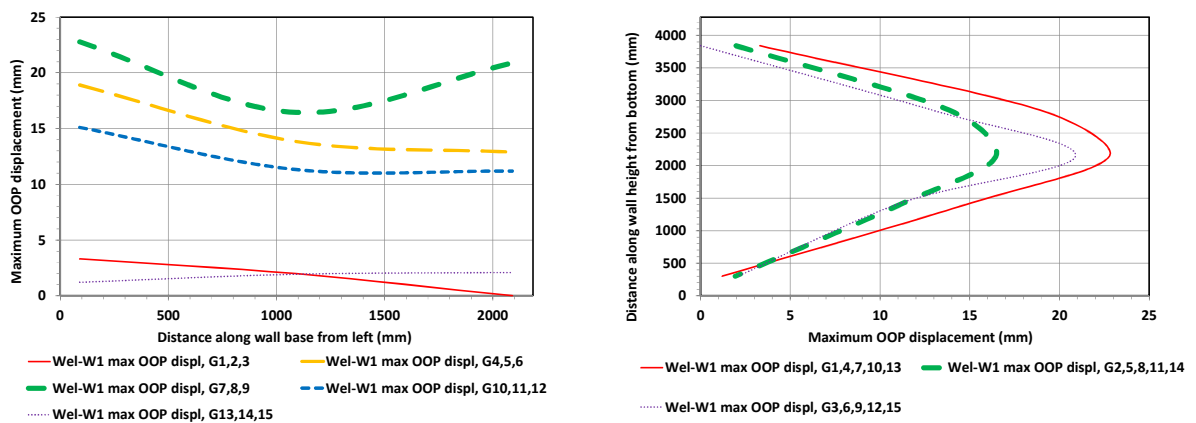
(a) Wel-W1 horizontal displacement profiles

(b) Wel-W1 vertical displacement profiles

Figure 30 continues on the following page
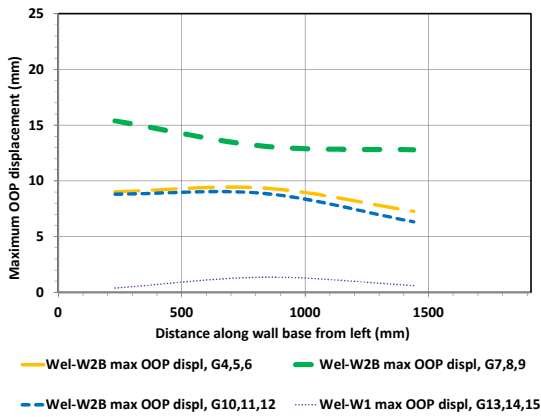
(c) Wel-W2B horizontal displacement profiles

(d) Wel-W2B vertical displacement profiles

(e) Wel-W3 horizontal displacement profiles

(f) Wel-W3 vertical displacement profiles

(g) Wel-W4 horizontal displacement profiles

(h) Wel-W4 vertical displacement profiles

Figure 30 continues on the following page

35

(i) Wel-W6 horizontal displacement profiles

(j) Wel-W6 vertical displacement profiles
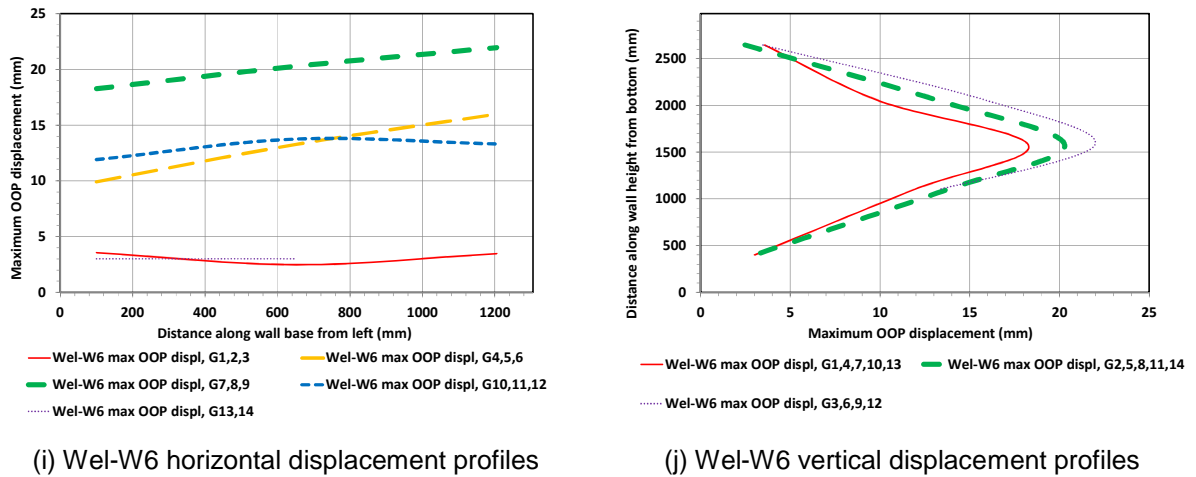
Figure 30: OOP maximum displacement profiles for walls tested in one-way vertical flexure at the WRS building

5.1.3   Crack patterns of walls tested in one-way vertical flexure

With the exception of Wel-W3, all walls tested in one-way vertical flexure in this program (i.e., those listed in **Tabl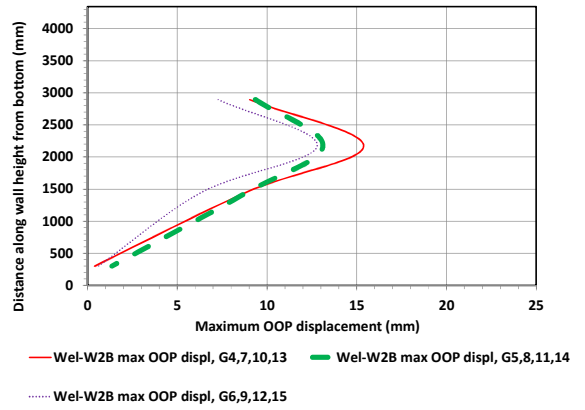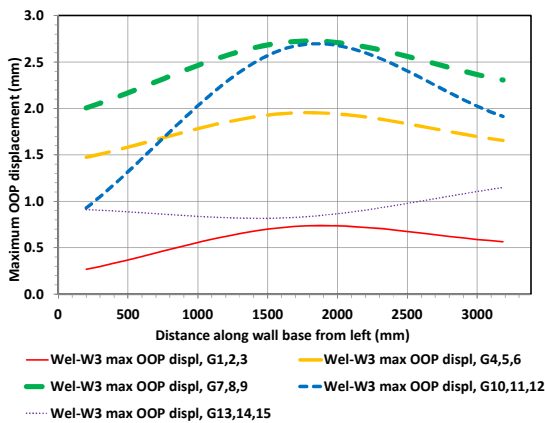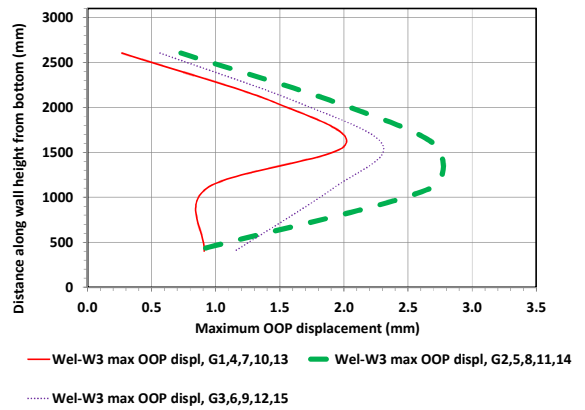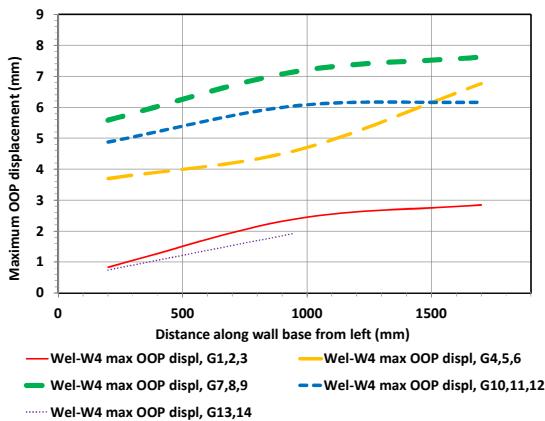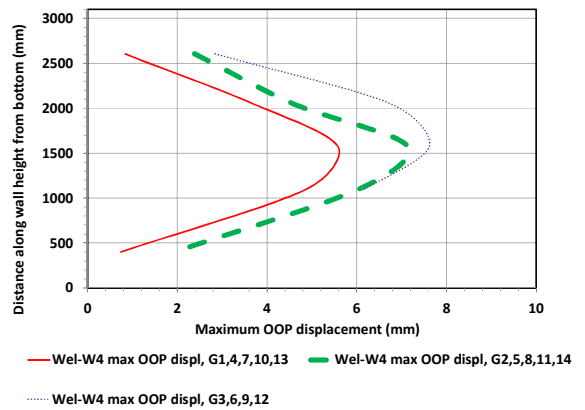e 9**) were loaded until a horizontal crack was formed across the entire length on the instrumentation side of each wall near mid-height. Corresponding to the locations of the maximum bending moments in **Figure 27**, horizontal cracks would initially form on the loaded side of each test wall near the base (and near the top in the case of walls fixed at the top) prior to the horizontal cracks forming near mid-height on the instrumentation side. The location of the horizontal cracks near mid-height also corresponded to the locations of maximum mid-span bending moments shown in **Figure 27** (i.e., cracks formed near one-half height in the case of walls fixed at the top and near five-eighths height in the case of walls propped at the top). The formation of mid-height horizontal cracks indicated that the response of the OOP walls tested in one-way vertical flexure transitioned from behaving as beams to behaving as rocking-wall mechanisms with mid-height hinges (see **Figure 28**). This rocking-wall behaviour forms the basis of the OOP ultimate displacement analysis procedure recommended for URM walls by Derakhshan et al. (2013a, 2014). These cracks closed partially after the load was released in each case. **Figure 31** includes images of typical horizontal cracks observed in this test program. Note that the height of each mid-height crack above the test wall base is an important value for assessment as discussed in **Section 5.1.4**.

(a) Horizontal crack near the bottom on the loaded side of Wel-W2B (marked for emphasis)
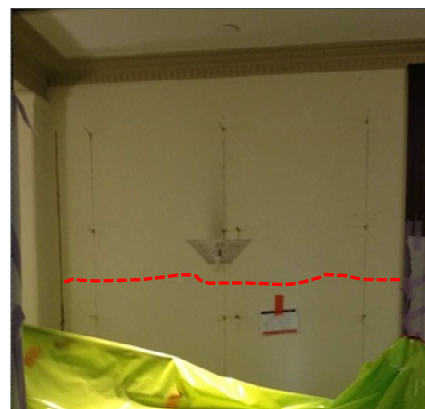
(b) Horizontal crack near one-half height on the instrumentation side of Wel-W4 (marked for emphasis)

Figure 31 continues on the following page
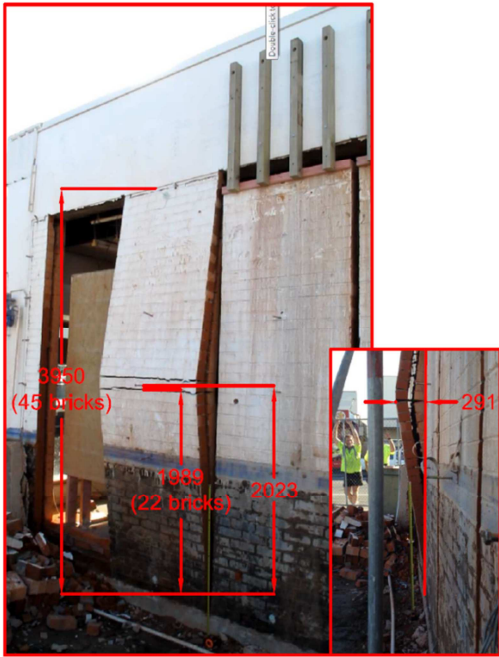
(c) Horizontal crack near one-half height on the instrumentation side of Has-W2 (example of use of photogrammetry to determine instability drift)
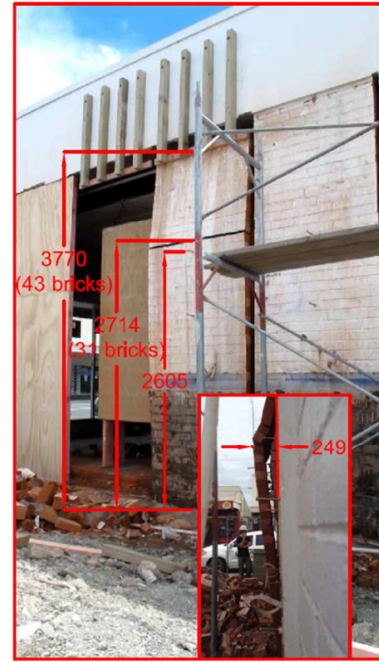
(d) Horizontal crack near five-eighths height on the instrumentation side of Has-W4 (example of use of photogrammetry to determine instability drift)

(e) Horizontal crack near five-eighths height on the instrumentation side of Auc-W1B (example of use of photogrammetry to determine instability drift)

(f) Horizontal crack near five-eighths height on the instrumentation side of Auc-W3 (example of use of photogrammetry to determine instability drift)

Figure 31: Crack patterns on selected walls tested in one-way vertical flexure

5.1.4 Flexural capacity and effective seismic loading capacity of walls tested in one-way vertical flexure

The g-force values shown in **Figure 29** for walls tested in one-way vertical flexure must be converted to represent uniformly distributed earthquake loads over the full-height walls (the process for which is described in **Section 4.1**). The results of this conversion from the test scenario to the assessment scenario for walls tested in one-way vertical flexure are summarised in **Table 10**. Note that the "pivot point" in the conversion from test wall to in situ wall is the maximum flexural capacity of each wall at a given cross-section.

Table 10: Summary of converting measured loads from test scenario to load capacities in seismic assessment scenarios (for walls tested in one-way vertical flexure)

Test ID	Top edge restraint condition	Test walls at partial, saw-cut height and with partially distributed test loads					Full-height walls with full-height, uniformly distributed effective loads				
		Max load (kN)*	Partial-height uniformly distributed load causing max flexural moment (kN/m)	Crack height above bottom of saw cut, if applicable (mm)	Crack height ratio, if applicable	Max flexural moment at crack height, if applicable, or mid-height (kNm/m)**	Full height of wall (mm)	Effective full-height uniformly distributed load causing max flexural moment (kN/m)***	Weight of wall full-height (kN)	Effective force-based capacity of full-height wall (g)
Wel-W1	Conf.	16.11	7.86	2300	0.54	2.32	4280	6.62	18.16	**1.56**
Wel-W2B	Conf.	13.54	6.60	2090	0.48	2.30	4342	5.60	16.97	**1.43**
Wel-W3	Conf.	40.35	19.68	n/a	n/a	1.74****	3100	14.72	20.77	**2.20**
Wel-W4	Conf.	42.08	20.53	1460	0.60	2.39	3100	11.35	11.66	**3.02**
Wel-W6	Unconf.	7.63	3.72	1470	0.61	1.13	2980	2.37	7.63	**0.93**
Has-W1	Conf.	16.44	8.02	2092	0.53	3.82	3950	7.06	17.36	**1.61**
Has-W2	Conf.	11.88	5.80	1989	0.50	2.79	3950	5.15	17.36	**1.17**
Has-W3	Unconf.	4.49	2.19	2714	0.72	1.37	3950	1.50	17.36	**0.34**
Has-W4	Unconf.	4.29	2.09	2714	0.72	1.31	3950	1.43	17.36	**0.32**
Has-W5	Conf.	10.16	4.96	2417	0.61	2.01	3950	3.71	17.36	**0.84**
Has-W6	Conf.	21.07	10.28	1884	0.48	4.90	3950	9.04	17.36	**2.06**
Auc-W1A	Unconf.	4.13	2.02	1891	0.70	0.78	3020	1.45	13.15	**0.33**
Auc-W1B	Unconf.	5.51	2.69	1891	0.70	1.03	3020	1.93	13.15	**0.44**
Auc-W2	Unconf.	4.04	1.97	1970	0.73	0.72	3020	1.35	13.15	**0.31**
Auc-W3	Unconf.	3.39	1.66	1733	0.64	0.67	3020	1.25	13.15	**0.29**

* max capacity of test wall limited by capacity of test frame or instrumentation in some cases

** solved using ETABS, http://civilengineer.webinfolist.com/fb/fbcalcu.php, or http://bendingmomentdiagram.com/pro-solve

*** http://www.awc.org/pdf/DA6-BeamFormulas.pdf

**** Wel-W3 did not exhibit any prominent horizontal cracks during testing, unlike the other walls listed in this table, due to limitation of the test frame, so this measured capacity may be less than the wall's actual maximum capacity, and the crack height was assumed to equal one-half of the test wall height.

Note that the three walls tested in the WRS building that were fixed at the top and successfully cracked at mid-height during loading (Wel-W1, Wel-W2B, and Wel-W4) as listed in **Table 10** were determined to have nearly identical flexural capacities (kNm/m), which is to be expected from walls in the same building with similar single-leaf wall thicknesses and material properties (It is probable that test wall Wel-W3 would have had a similar flexural capacity had it been successfully loaded so as to create a mid-height crack.) Note that test wall Wel-W4 is expected to have a much higher effective force-based capacity due to its significantly shorter full-height as compared to its counterparts Wel-W1 and Wel-W2B.

Considering that the walls tested in one-way vertical flexure at the Hastings and Auckland CBD buildings were similar in geometry (length and two-leaf thickness with a cavity), various trends are charted in **Figure 32** considering the cavity tie spacings listed in **Table 9**, the instability drifts charted in **Figure 29**, and the effective force-based capacities listed in **Table 10**. Note that test walls Has-W3 and Auc-W1B had the same cavity ties installed at the same vertical spacing, as well as propped top conditions. Because test wall Has-W3 was thicker (see **Table 9**), test wall Auc-W1B benefitted from stronger material properties in order to be loaded to both a higher capacity and instability drift than Has-W3 (see **Section 3.1**).
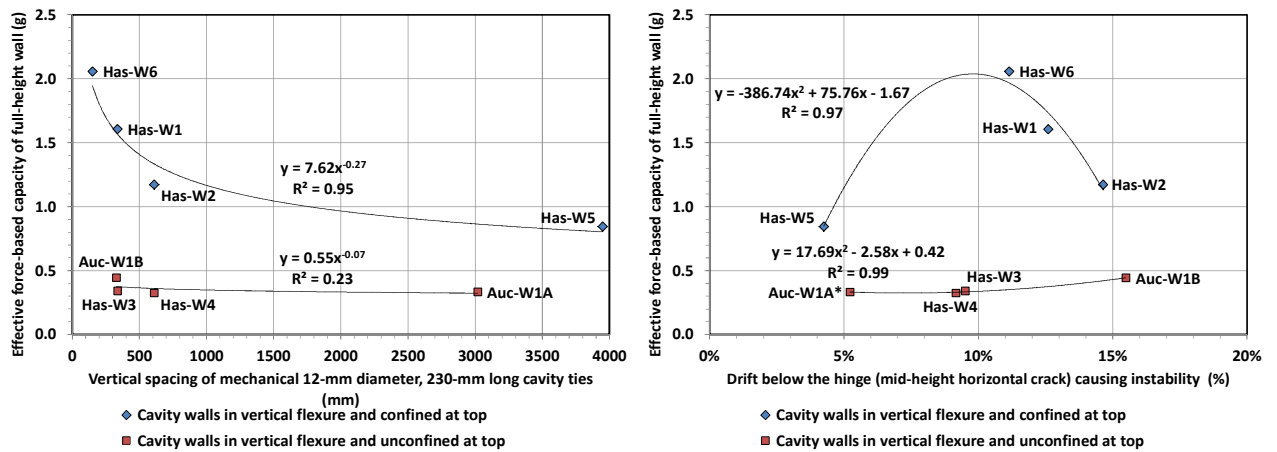
(a) Vertical spacing of cavity ties (mm) versus effective capacity (g) with trend lines

(b) Instability drift (%) versus capacity (g) for walls with different cavity tie spacings with trend lines (*The value of instability drift was estimated for Auc-W1A based on the relative performance of other walls.)

Figure 32: Retrofitted cavity wall trends

The trend lines in **Figure 32** indicate a strong correlation between reduced cavity tie spacing and increased load capacity for walls with topside fixed restraint condition. As previously indicated in **Figure 29(l)**, however, reduced cavity tie spacing and increased strength eventually correlate with a reduction in displacement capacity. Walls with propped tops are less sensitive to changes in cavity tie spacing in regard to load capacity, although displacement capacity may still be greatly improved. The authors theorise that walls with fixed restraint conditions on both top and bottom edges benefit more from cavity tie retrofitting due to the "arching" force that must be transmitted across the cavity, whereas walls with propped tops need only transfer the wall dead weight across the cavity.

Seismic assessment procedures formally utilised in New Zealand entail a scoring system of percent New Building Standard (%NBS) as proposed by NZSEE (2006), which indicates the expected capacity of the building as a percentage of the ultimate limit state (ULS) demands prescribed by the current loading standard (NZS 1170.5:2004). The phrase "new building standard" is indicative of the intent of the scoring system - a building that is assessed as having a resistance exceeding 100%NBS is expected to

withstand the current ULS "design basis earthquake" (DBE) demands, whereas a building assessed at 33%NBS is expected to withstand only one-third of the DBE. A building with a score of less than 33%NBS is deemed "earthquake prone" and is potentially subject to regulatory measures per the Building Act (New Zealand Parliament 2004) and, in most cases, the Territorial Authority's policy warranting further assessment and possibly structural retrofits. A building with a score less than 67%NBS is deemed "earthquake risk" and is potentially subject to the provisions of the Health and Safety in Employment Act (New Zealand Parliament 1992). Note that the earthquake defined by the loadings standard (NZS 1170.5 2004) as the DBE for any particular building is influenced by a number of factors, including the location, site conditions, and functional purpose of the building being considered. Note also that the correlation between %NBS ratings determined for existing, older buildings and those determined for newly designed buildings can be skewed by, amongst other factors, differences in characteristic strengths presumed and factors of safety utilised (Au et al. 2013).

The relative hazard factor Z in NZS 1170.5:2004 is effectively equivalent to S_a in ASCE/SEI 7-10 (2010). The hazard factor for Hastings is Z = 0.39, which is amongst the higher values for any of New Zealand's major cities when considering that Z = 0.13 applies in Auckland (the country's most populated city) and Z = 0.40 applies in Wellington (the country's capital) (NZS 1170.5:2004). Considering these relative hazards, the %NBS results for four different assessment scenarios are summarised in **Table 11** for all of the walls tested in one-way vertical flexure in this program.

Table 11: Summary of %NBS from converting measured loads from test scenario to load capacities in seismic assessment scenarios (for walls tested in one-way vertical flexure, assuming shallow soils)

| Test ID | Top edge restraint condition | %NBS based on effective force-based capacity and NZS 1170.5:2004 "Parts and Components" demands* | | | | | | | |
| | | Auckland, ground floor of 4.5-m tall building | | Auckland, third floor of 12-m tall building | | Wellington, ground floor of 4.5-m tall building | | Wellington, third floor of 12-m tall building | |
		Demand (g)	%NBS	Demand (g)	%NBS	Demand (g)	%NBS	Demand (g)	%NBS
Wel-W1	Conf.	0.47	332%	0.99	158%	1.44	108%	3.04	51%
Wel-W2B	Conf.	0.47	304%	0.99	145%	1.45	99%	3.04	47%
Wel-W3	Conf.	0.44	505%	0.95	230%	1.34	164%	2.93	75%
Wel-W4	Conf.	0.44	694%	0.95	316%	1.34	225%	2.93	103%
Wel-W6	Unconf.	0.43	214%	0.95	97%	1.33	70%	2.92	32%
Has-W1	Conf.	0.46	349%	0.98	164%	1.41	114%	3.01	53%
Has-W2	Conf.	0.46	255%	0.98	120%	1.41	83%	3.01	39%
Has-W3	Unconf.	0.46	74%	0.98	35%	1.41	24%	3.01	11%
Has-W4	Unconf.	0.46	71%	0.98	33%	1.41	23%	3.01	11%
Has-W5	Conf.	0.46	184%	0.98	86%	1.41	60%	3.01	28%
Has-W6	Conf.	0.46	447%	0.98	210%	1.41	145%	3.01	68%
Auc-W1A	Unconf.	0.43	77%	0.95	35%	1.33	25%	2.93	11%
Auc-W1B	Unconf.	0.43	103%	0.95	47%	1.33	33%	2.93	15%
Auc-W2	Unconf.	0.43	72%	0.95	33%	1.33	23%	2.93	11%
Auc-W3	Unconf.	0.43	67%	0.95	30%	1.33	22%	2.93	10%

* max capacity of test wall limited by capacity of test frame or instrumentation in some cases

Where the test walls were able to be loaded to collapse (in Hastings and the Auckland CBD buildings) and the instability drifts could be determined, the natural period of the representative system, T_p, was determined in accordance with Derakhshan et al. (2014). The average calculated natural periods for test walls fixed and propped at the top were 0.37 and 0.70 seconds, respectively. With the highest calculated natural period for any single test wall being 0.74 seconds, it was assumed that all test walls, including those not loaded to collapse in the WRS building, would have a part spectral shape coefficient, $C_i(T_p)$ = 2.0 (NZS 1170.5:2004). Assuming a shallow subsoil site class, non-ductile OOP behaviour of the wall (which is appropriate for a peak force-based assessment based on the behaviour indicated in **Figure 29** for most walls), a part risk factor, R_p = 1.0, a building importance level of 2 (representing a normal building, and hence, warranting the consideration of a DBE with an average return period of 1 in 500 years), and the wall geometries and densities listed in **Table 9**, the %NBS for each of the test walls was able to be determined for each of four scenarios as summarised in **Table 11**. Please note when considering these %NBS values that an inherent conservativeness exists within both force-based assessments and one-way vertical flexural analyses.

5.2   Walls tested in two-way flexure

Within the entire test program, six distinct test wall panels were tested once each in two-way flexure. The geometries of those walls are summarised in **Table 12**. Note that the total thickness without ("w/o") including the cavity width represents the thickness of two bricks in the case of the two-leaf cavity wall and is considered in this fashion for purposes of determining wall weights. Except where indicated in **Table 12**, masonry density was based on dimensional measurements and weighting, as noted in **Section 3.1**.

Table 12: Summary of geometry of walls tested in two-way flexure

Test ID	# brick leaves	Bottom edge restraint condition	Top edge restraint cond.	Length (mm)	Test height (mm)	Mean masonry density (kg/m³)	Total thickness of wall w/o cavity (mm)	Total thickness of wall incl. cavity (mm)	Cavity tie
Wel-W2A	1	Conf.	Conf.	2662	4342	1926**	108	108	n/a
Wel-W5	1	Conf.	Unconf.	2580	2980	1884**	108	108	n/a
Ora-W1	2, cavity	Free*	Conf.	3346	2940	1783**	218	268	In situ
Ora-W2	1	Free*	Conf.	3380	2655	1783**	109	109	n/a
Auc-W4	1	Conf.	Conf.	4400	3400	1720	114	112.5***	n/a
Auc-W5	1	Conf.	Conf.	4400	3400	1720	114	112.5***	n/a

* Bottom edge effectively unrestrained on Ora-W1 and Ora-W2 due to horizontal saw cut; however, the exterior leaf of Ora-W1 was not saw cut but rested on a smooth lead damp-proof sheeting course

** Stacked masonry prism elements (consisting of multiple bricks and mortar joints intact) were not able to be extracted from the WRS building nor the Orakei building. Hence, the density in this case was determined based on the brick and mortar compression strengths as explained in **Section 3.1**.

*** Exterior leaf of Auc-W4 and Auc-W5 removed prior to testing

5.2.1   Load-displacement response of walls tested in two-way flexure

As with the walls tested in one-way vertical flexure, all walls tested in two-way flexure were loaded semi-cyclically at a quasi-static loading rate. The left vertical axes in **Figure 33** represent the total test load (i.e., combination of loads measured by all of the individual load cells) divided by the weight of each wall, expressed as a result in terms of horizontal acceleration (g). The test wall geometries and masonry material densities used to determine the horizontal acceleration capacity of each wall are listed in **Table 12**. Unlike in the case of the walls tested in one-way vertical flexure, the test heights were equivalent to the full-heights in the case of walls tested in two-way flexure. With the loaded areas being smaller than the total areas of the walls tested in two-way flexure, and with the loaded areas being concentrated near the centres of the test walls, the accelerations (g) shown in **Figure 33** are likely to be conservative. Test

41

wall Auc-W5 was able to be loaded to OOP collapse, but as the collapse occurred gradually (in contrast to walls tested in one-way vertical flexure), the instability drift was not clearly defined.
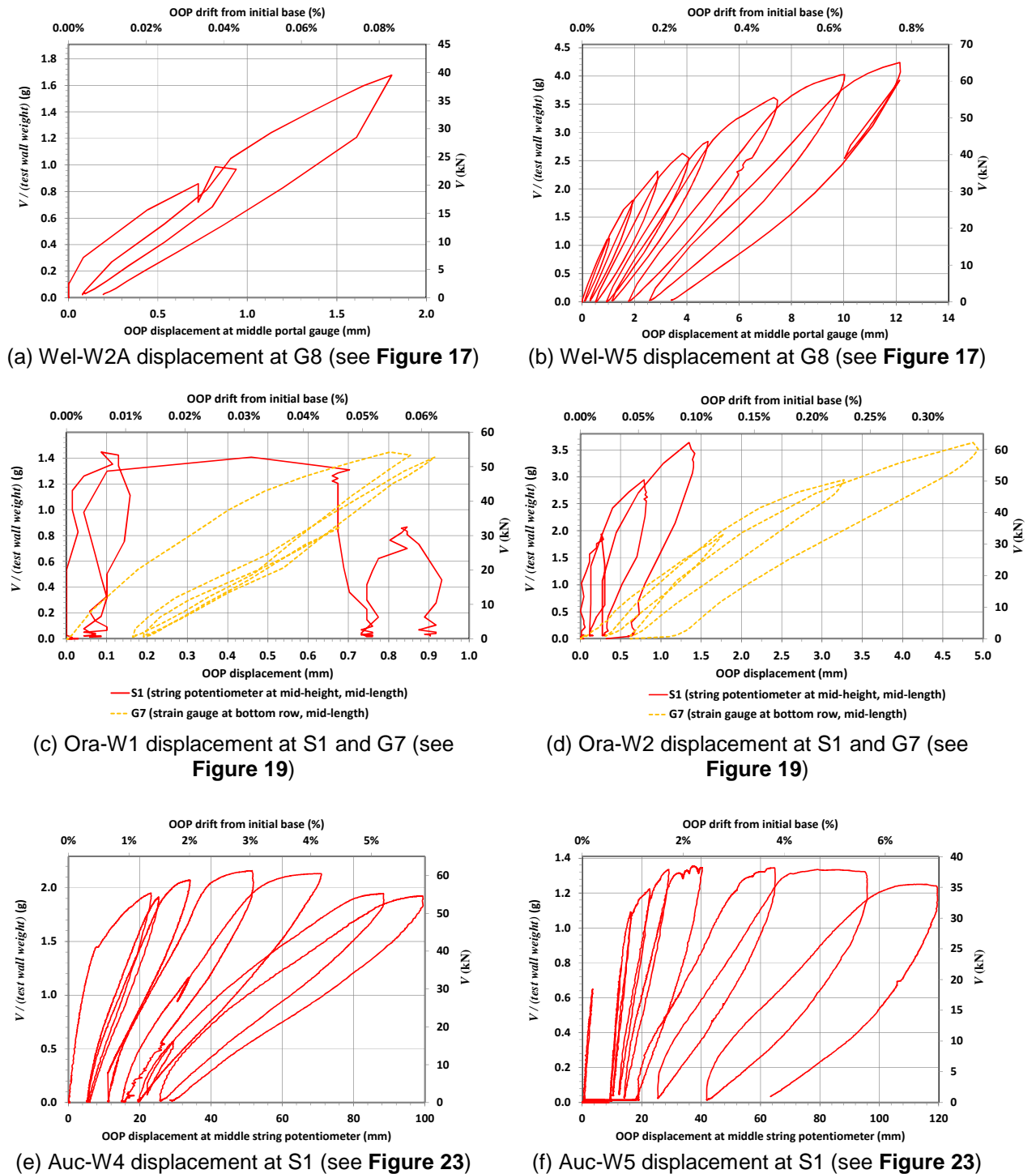

(a) Wel-W2A displacement at G8 (see **Figure 17**)

(b) Wel-W5 displacement at G8 (see **Figure 17**)

(c) Ora-W1 displacement at S1 and G7 (see **Figure 19**)

(d) Ora-W2 displacement at S1 and G7 (see **Figure 19**)

(e) Auc-W4 displacement at S1 (see **Figure 23**)

(f) Auc-W5 displacement at S1 (see **Figure 23**)

Figure 33: Load-displacement responses for walls tested in two-way flexure

The following comments should be considered in conjunction with the force-displacement plots shown in **Figure 33**:

◗ The tests wall at the WRS and Orakei buildings needed to be reinstated after testing and so could not be loaded until collapse;

42

- Wall Wel-W2A was loaded until the capacity of the load frame was reached, which occurred at a very low OOP wall displacement (and hence high stiffness). The load-displacement curve [see **Figure 33(a)**] does not appear to be plateauing at all, leaving researchers to conclude that the wall had additional load capacity above what was measured;

- Wall Wel-W5 was loaded until the capacity of the load cell instrumentation was reached. The load-displacement curve in **Figure 33(b)** for wall Wel-W5 appears close to plateauing and is hence considered to be approximately representative of the peak load capacity of the test wall;

- Walls Ora-W1 and Ora-W2 – effectively in double flexure with a mostly free bottom edge – were loaded until the capacity of the load cell instrumentation was reached. No cracking was observed in either test wall. Hence, the maximum loads applied to the wall as shown in **Figure 33(c)** and **(d)** are likely less than the respective load capacities of the two walls;

- The interior leaf of wall Ora-W1 was loaded with all force transfer to the outer leaf occurring through the in situ 4 mm diameter steel ties. Tie material plastic deformation or permanent shear slippage within the mortar joints likely contributed to the high initial stiffness as well as the high residual OOP displacements observed at the instrument S1 location [see **Figure 33(c)**] at the mid-height, mid-length of the test wall. Where ties were less prominent, and hence, less influential at the instrument G7 location at the effectively free bottom and mid-length of the wall, residual deformation was greatly reduced, and the wall OOP behaviour exhibited more common self-centring characteristics;

- Similar to wall Ora-W1, wall Ora-W2 exhibited very high initial stiffness near the instrument S1 location [see **Figure 33(d)**] at the mid-height, mid-length of the test wall. Due to its single-leaf thickness, wall Ora-W2 experienced higher OOP displacements under similar loads than did the two-leaf wall Ora-W1, particularly at the instrument G7 location at the effectively free bottom and mid-length of the wall; and

- The disparity between the behaviours of the two walls tested in two-way flexure at the Auckland CBD building [see **Figure 33(e)** and **(f)**] indicates that pre-existing in-plane damage can significantly reduce the OOP load capacity of a URM infill wall, although such damage may not necessarily limit the displacement capacity.

5.2.2   Displacement profiles of walls tested in two-way flexure

The horizontal and vertical maximum displacement profiles for all walls tested in two-way flexure are shown in **Figure 34**. Note the eccentricity present in the walls tested at the WRS building [see **Figure 34(a)** – **(d)**] due to the presence of a thickened pier and a return wall on walls Wel-W2A and Wel-W5, respectively. Also note that wall Wel-W2A was loaded eccentrically due to onsite restraints and the desire to maintain a consistent load point between Wel-W2A and Wel-W2B (the latter of which was tested in one-way vertical flexure after the wall was vertically cut on both sides following the testing of Wel-W2A).

Figure 34(e) – **(h)** show the horizontal and vertical maximum displacement profiles for both test walls in the Oraekie building. Due to the smoothed lines used in the charts and the inclusion of the value from instrument S2 only in the vertical displacement profiles, the apparent difference in maximum displacement illustrated by the charts in **Figure 34(e)** and **(f)** for test wall Ora-W1 is artificial [see **Figure 33(c)**]. Furthermore, instrument G5 on test wall Ora-W1 and instrument G2 on test wall Ora-W2 did not provide reliable data during testing, so the values indicated in **Figure 34** for these instruments were estimated based on other instrumentation.

Other than for the Orakei test walls which were cut horizontally along the base, most of the vertical displacement profiles in **Figure 34** appear to trend toward zero maximum displacement at the boundaries, suggesting a high shear rigidity and capacity at these locations. As a counterexample, the

43

horizontal displacement profiles for Ora-W1 and Ora-W2 as measured by instrumentation at mid-height (i.e., G4, S1, G5) in **Figure 34(e)** and **(g)** do not appear to trend toward zero maximum displacement at the vertical edges of the walls, suggesting that some small amount of deformation may have occurred at the vertical interfaces between the RC columns and the brick infill walls, albeit under relatively large loads.
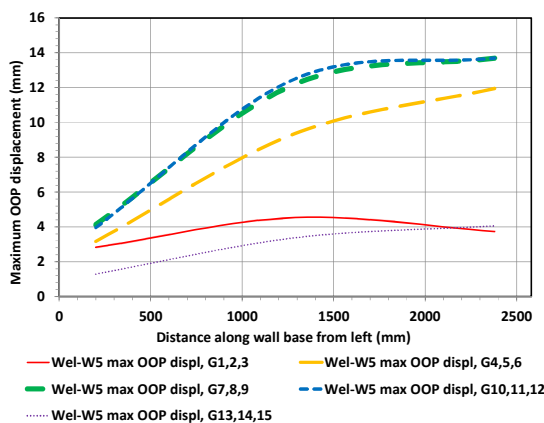
Finally, note the unique effect that simulating in-plane cracking had on the displacement profiles near the horizontal boundaries for test wall Auc-W5 [see **Figure 34(l)**] as compared to its undamaged counterpart Auc-W4 [see **Figure 34(k)**].
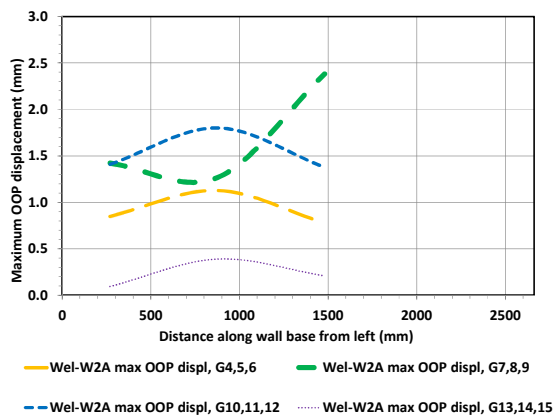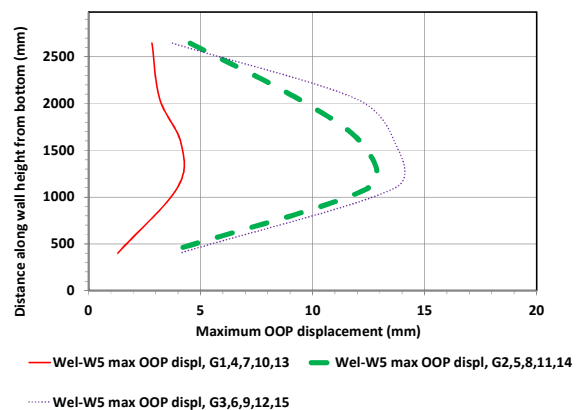

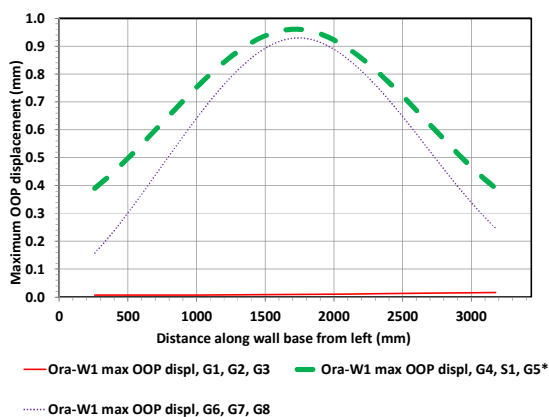(a) Wel-W2A horizontal displacement profiles
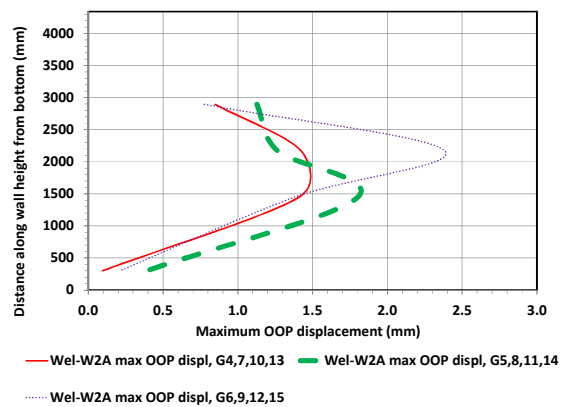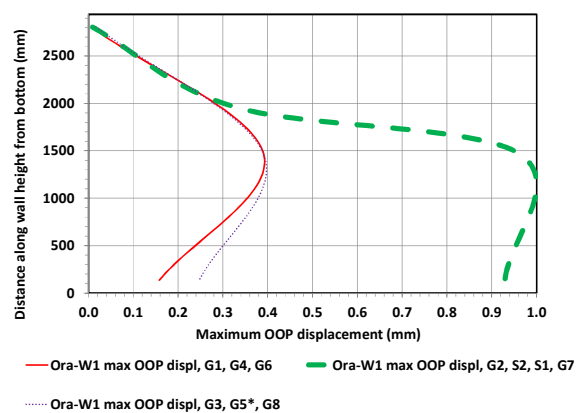

(b) Wel-W2A vertical displacement profiles

(c) Wel-W5 horizontal displacement profiles

(d) Wel-W5 vertical displacement profiles
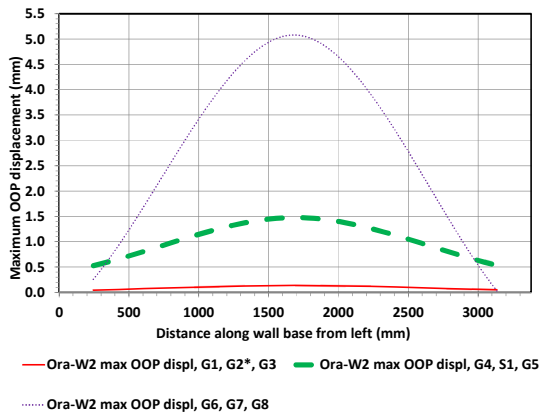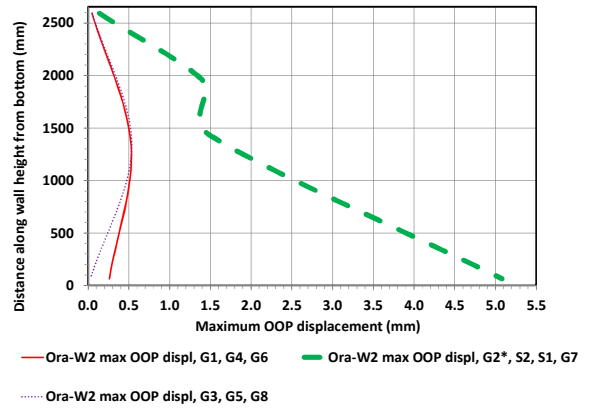

(e) Ora-W1 horizontal displacement profiles
(* indicates estimated displacement)

(f) Ora-W1 vertical displacement profiles
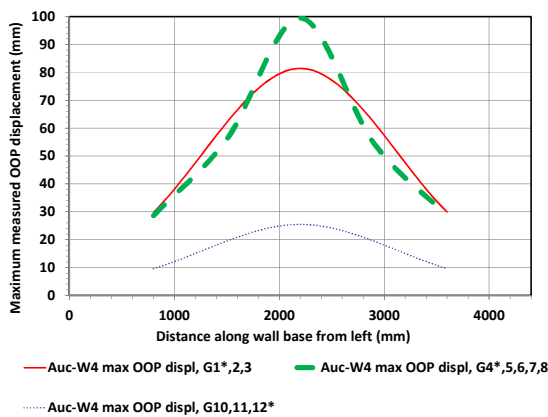(* indicates estimated displacement)

Figure 34 continues on the following page

44

(g) Ora-W2 horizontal displacement profiles
(* indicates estimated displacement)

(h) Ora-W2 vertical displacement profiles
(* indicates estimated displacement)

(i) Auc-W4 horizontal displacement profiles
(* indicates estimated displacement)

(j) Auc-W4 vertical displacement profiles
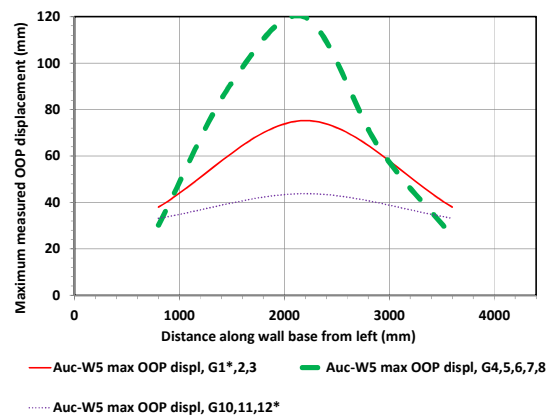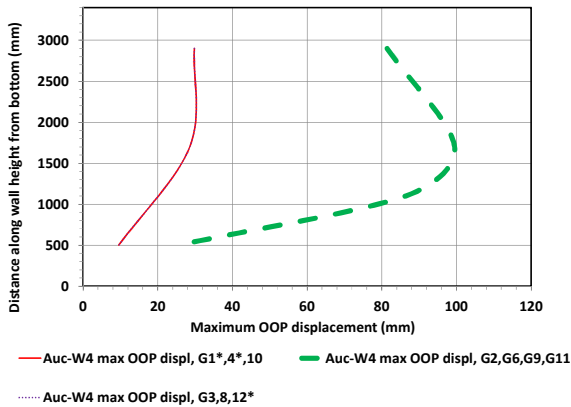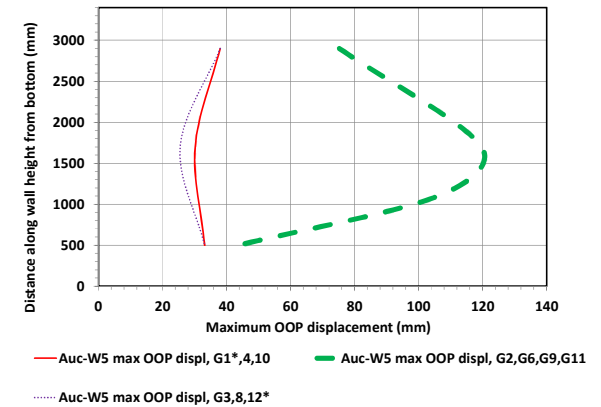(* indicates estimated displacement)

(k) Auc-W5 horizontal displacement profiles
(* indicates estimated displacement)

(l) Auc-W5 vertical displacement profiles
(* indicates estimated displacement)

Figure 34: OOP maximum displacement profiles for walls tested in two-way flexure

5.2.3 Crack patterns of walls tested in two-way flexure

Most wall tested in two-way flexure in this program were not capable of being severely damaged. However, the walls tested at the Auckland CBD building (see **Figure 35**) serve as good visual examples of the damage that typically occurs in two-way flexure, consistent with analysis assumptions in masonry design standards (e.g., AS 3700:2011).

Corresponding to the locations of the maximum bending moments in **Figure 27** and consistent with observations of initial crack formation on walls tested in one-way vertical flexure, horizontal cracks would initially form on the loaded side of each test wall near the fixed boundaries prior to the proliferation of cracks across the midsections of the walls. Note that, as shown in **Figure 35(a)**, cracks on the instrumentation side formed in test wall Auc-W4 (which was initially undamaged) in two planes in a similar fashion to those intentionally created in Auc-W5 [see **Figure 13(c)**].

(a) Crack pattern post-loading on the instrumentation side of Auc-W4

(b) Crack pattern post partial loading on the instrumentation side of Auc-W5

(c) Crack pattern post-loading on the loading side of Auc-W4

(d) Partial wall collapse post-loading on the loading side of Auc-W5

Figure 35: Cracking and partial collapse on test walls Auc-W4 and Auc-W5

5.2.4 Flexural capacity and effective seismic loading capacity of walls tested in two-way flexure

Consistent with the assumptions for computing load demands from the "parts and components' section of the New Zealand loading standard (NZS 1170.5:200), the walls tested in two-way flexure were also assessed for force-based capacity in units of horizontal seismic acceleration (g) and %NBS, with the results summarised in **Table 13** and **Table 14**. Since all walls tested in two-way flexure were tested in their full-height condition with loading concentrated near the centre of each wall, the results below are assumed to be slightly conservative. Furthermore, recall that many of these walls were not able to be tested to their maximum capacities.

Table 13: Summary of load capacities of walls tested in two-way flexure

Test ID	# brick leaves	Length (mm)	Test height (mm)	Total brick thickness (m)	Maximum test load (kN)*	Weight of wall full-height (kN)	Test force-based capacity (g)*
Wel-W2A	1	2662	4342	108	41.64	23.59	1.77
Wel-W5	1	2580	2980	108	65.13	15.34	4.25
Ora-W1	2, cavity	3346	2940	228	57.23	39.60	1.45
Ora-W2	1	3380	2655	114	63.93	18.06	3.54
Auc-W4	1	4400	3400	112.5	61.29	28.40	2.16
Auc-W5	1	4400	3400	112.5	38.44	28.40	1.35

* max capacity of test wall limited by capacity of test frame or instrumentation in some cases

Table 14: Summary of %NBS comparing loads from test scenario to load capacities in seismic assessment scenarios (for walls tested in two-way vertical flexure, assuming shallow soils)

Test ID	# brick leaves	%NBS based on effective force-based capacity and NZS 1170.5:2004 "Parts and Components" demands*							
		Auckland, ground floor of 4.5-m tall building		Auckland, third floor of 12-m tall building		Wellington, ground floor of 4.5-m tall building		Wellington, third floor of 12-m tall building	
		Demand (g)	%NBS	Demand (g)	%NBS	Demand (g)	%NBS	Demand (g)	%NBS
Wel-W2A	1	0.47	375%	0.99	178%	1.45	122%	3.04	58%
Wel-W5	1	0.43	983%	0.95	447%	1.33	320%	2.92	145%
Ora-W1	2, cavity	0.43	336%	0.95	152%	1.32	109%	2.92	49%
Ora-W2	1	0.42	838%	0.94	376%	1.30	272%	2.90	122%
Auc-W4	1	0.44	486%	0.96	224%	1.37	158%	2.96	73%
Auc-W5	1	0.44	305%	0.96	141%	1.37	99%	2.96	46%

* max capacity of test wall limited by capacity of test frame or instrumentation in some cases

6.   Conclusions and Recommendations

Significant results that can be drawn from this research program are as follows:

◗ Restraint at the walls' vertical edges (horizontal boundaries), resulting in two-way OOP flexure as compared to one-way vertical OOP flexure, can substantially improve the OOP load-carrying capacity of tested infill walls;

◗ Topside fixed restraint and presumed "arching" action from the building frame can greatly increase the out-of-plane capacity of infill walls;

◗ In-plane damage can significantly reduce the out-of-plane capacity of a URM infill wall;

◗ Retrofit ties with adequate spacing and shear stiffness can greatly improve the out-of-plane capacity of URM cavity walls. For a force-based analysis in one case-study, the wall strip strength was approximately doubled from the in situ condition to the condition in which ties were vertically spaced at approximately 150 mm. An even greater improvement in displacement-based performance was observed;

◗ The relative behaviour of the cavity walls tested in vertical flexure as well as visual observation of the failure mechanisms led the researchers to conclude that, if cavity tie spacing was held constant, then cavity tie diameter was the most important difference in the relative performance of the retrofitted cavity walls (as opposed to differences in model or installation mechanism), which is logical given the relationship between cavity tie diameter and shear flow capacity. Adhesive cavity ties were not notably more useful to improving OOP cavity wall performance than were more easily inserted mechanical cavity ties;

◗ Increasing too greatly the OOP stiffness and strength of a wall spanning between rigid concrete elements can reduce its ultimate displacement capacity; and

◗ Material strengths related to brick compression, mortar compression, masonry bed joint shear, cavity tie pull-out, as well as other properties have been determined for a range of buildings in this typology, resulting in the ability for consulting engineers to make more accurate assumptions while performing building analyses in the future.

6.1   Recommended numerical assessment techniques

If the results pertaining to walls tested in double flexure need to be considered further, the authors recommend referencing analysis techniques in accordance with the Australian design standard (Griffith and Vaculik 2007; AS 3700-2011; Think Brick 2013) with material properties and boundary conditions adjusted accordingly. AS 3700-2011 utilises a virtual work-based, two-way flexural analysis, to include weighted components of horizontal flexure (i.e., flexure about a vertical axis) and diagonal flexure. Griffith and Vaculik (2007) validated the relative accuracy of the AS 3700:2011 method with empirical testing, provided that return walls were assumed to provide only partial moment restraint such that the vertical edge restraint factor, R_f, equalled 0.5.

A displacement-based assessment may be warranted to improve the assessed performance of walls tested in single-axis vertical flexure (e.g. Derakhshan et al. 2013a, 2014). Please note, however, that the spectral demands may need to be reassessed. While the NZS 1170.5:2004 spectrum represents the current standard in New Zealand, it is based on the following assumptions and scenarios pertaining to the building (Shelton 2004):

◗ structure comprised of steel and/or concrete;

◗ buildings 3, 10, or 20 storeys in height;

- ◗ ductility factor range of 3 to 6;

- ◗ inelastic behaviour included; and

- ◗ structural performance factor of 0.7.

These assumptions may not align with the assumptions considered by engineers for their buildings. Hence, Derakhshan et al. (2014) offer an alternative response spectrum for "parts and components" that is specific to unreinforced masonry components and may be more appropriate.

6.2 Recommended potential further testing

Further research in this area will involve advanced data processing to more accurately define the effects of different boundary conditions on URM infill wall performance. Further testing will preferably involve an examination of more retrfoti techniques. Some walls, for example, may be retrofitted with vertical near surface mounted (NSM) carbon fiber (CFRP) strips installed which will provide a cost effective and minimally-invasive seismic retrofit technique, for some scenarios where cavity ties are not appropriate, particularly for walls that are propped at the tops.

6.3 Acknowledgements

The geometry and material specifications of the cavity wall ties that performed the most admirably in this research project are associated with a product that was available during the research investigation but is no longer currently available in New Zealand. As a result of the outcomes from this research program, Simpson Strong-Tie has agreed to invest in the market potential for this product and is currently manufacturing an cavity tie with similar specifications to the one utilised in this research program with the explicit intention of shipping inventory to New Zealand within the calendar year.

7. References

Almesfer, N.; Lumantarna, R.; Dizhur, D.; and Ingham, J. (2014). *Material Properties of Existing Unreinforced Clay Brick Masonry Buildings in New Zealand*. Bulletin of the New Zealand Society for Earthquake Engineering, 47(2).

AIUMBER (2012). *Assessment and Improvement of Unreinforced Buildings for Earthquake Resistance.* Faculty of Engineering, University of Auckland, New Zealand. http://masonryretrofit.org.nz/SARM/1.pdf

AS 3700-2011 (2011). *Australian Standard for Masonry Structures*. Standards Australia, Committee BD-004, Sydney, NSW, Australia.

ASCE/SEI 7-10 (2010). *Minimum Design Loads for Buildings and Other Structures*. American Society of Civil Engineers (ASCE), Reston, Virginia, United States.

ASTM C1072-11 (2011). *Standard Test Methods for Measurement of Masonry Flexural Bond Strength*. ASTM International, West Conshohocken, Pennsylvania, United States.

ASTM C1314-11a (2011). *Standard Test Method for Compressive Strength of Masonry Prisms*. ASTM International, West Conshohocken, Pennsylvania, United States.

ASTM C1531-03 (2003). *Standard Test Methods for In Situ Measurement of Masonry Mortar Joint Shear Strength Index.* ASTM International, West Conshohocken, Pennsylvania, United States.

ASTM C67-11 (2011). *Standard Test Methods for Sampling and Testing Brick and Structural Clay Tile*. ASTM International, West Conshohocken, Pennsylvania, United States.

Au, E.; Lomax, W.; Walker, A.; Banks, G.; and Haverland, G. (2013). *A Discussion on the Differences between New Zealand's Philosophy for the Seismic Design of New Buildings and Seismic Assessment of Existing Buildings, and the Issues that Arise*. Proc. of the New Zealand Society for Earthquake Engineering Conference, April: 26-28. Wellington, New Zealand.

Derakhshan, H.; Griffith, M.; and Ingham, J. (2013a). *Out-of-Plane Behaviour of One-Way Spanning URM Walls*. ASCE Journal of Engineering Mechanics, 139, 4, 409-417. http://dx.doi.org/10.1061/(ASCE)EM.1943-7889.0000347

Derakhshan, H.; Griffith, M.; and Ingham, J. (2013b). *Airbag Testing of Multi-Leaf Unreinforced Masonry Walls Subjected to One-Way Bending*. Engineering Structures, 57, 12, 512-522. http://www.sciencedirect.com/science/article/pii/S0141029613004665

Derakhshan, H.; Griffith, M.; and Ingham, J. (2014). *Seismic Assessment of Out-of-Plane Loaded Unreinforced Masonry Walls in Multi-Storey Buildings*. Bulletin of the New Zealand Society for Earthquake Engineering, 47(2).

Dizhur, D.; Ismail, N.; Knox, C.; Lumantarna, R.; and Ingham J.M. (2010). *Performance of Unreinforced and Retrofitted Masonry Buildings During the 2010 Darfield Earthquake*. Bulletin of the New Zealand Society for Earthquake Engineering. 43(4):321–39.

Dizhur, D.; Ingham, J.M.; Moon, L.; Griffith, G.M.; Schultz, A.; Senaldi, I.; Magenes, G.; Dickie, J.; Lissel, S.; Centeno, J.; Ventura, C.; Leite, J.; and Lourenco, P. (2011). *Performance of Masonry Buildings and Churches in the 22 February 2011 Christchurch Earthquake*. Bulletin of the New Zealand Society for Earthquake Engineering.

Dizhur, D. (2013). *Performance of Masonry Buildings in the Canterbury Earthquakes and Corresponding Strengthening Using NSM CFRP Strips.* Doctoral Dissertation, University of Auckland, Department of Civil and Environmental Engineering. http://hdl.handle.net/2292/19922

Dizhur, D.; Griffith, M.; and Ingham, J. (2014). *Out-of-Plane Strengthening of Unreinforced Masonry Walls Using Near Surface Mounted Fibre Reinforced Polymer Strips*. Engineering Structures, 59, 2, pp. 330-343. http://dx.doi.org/10.1016/j.engstruct.2013.10.026

Griffith, M.C. and Vaculik, J. (2007). *Out-of-Plane Flexural Strength of Unreinforced Clay Brick Masonry Walls*. The Masonry Society Journal, September: 53-68.

Ingham, J. and Griffith, M. (2011a). *The Performance of Unreinforced Masonry Buildings in the 2010/2011 Canterbury Earthquake Swarm.* Report to the Royal Commission of Inquiry. http://canterbury.royalcommission.govt.nz/documents-by-key/20110920.46

Ingham, J. and Griffith, M. (2011b). *The Performance of Earthquake Strengthened URM Buildings in the Christchuch CBD in the 22 February 2011 Earthquake.* Report to the Royal Commission of Inquiry. http://canterbury.royalcommission.govt.nz/documents-by-key/20111026.569

IPENZ (2014). *Engineering Heritage New Zealand - Wellington Railway Station.* Institution of Professional Engineers New Zealand, accessed 07 February. http://www.ipenz.org.nz/heritage/itemdetail.cfm?itemid=85

Lumantarna, R.; Biggs, D.T.; Ingham, J. M. (2014). *Uniaxial Compressive Strength and Stiffness of Field Extracted and Laboratory Constructed Masonry Prisms.* ASCE Journal of Materials in Civil Engineering. http://dx.doi.org/10.1061/(ASCE)MT.1943-5533.0000731

New Zealand Parliament (1992). *Health and Safety in Employment Act.* Date of assent: 27 October. Department of Labour, New Zealand Government, Wellington, New Zealand.

New Zealand Parliament (2004). *Building Act.* Department of Building and Housing – Te Tari Kaupapa Whare, Ministry of Economic Development, New Zealand Government, Wellington, New Zealand.

NZHPT (2014). *The Register - Wellington Railway Station.* New Zealand Historic Places Trust, accessed 07 February. http://www.historic.org.nz/TheRegister/RegisterSearch/RegisterResults.aspx?RID=1452

NZS 1170.5:2004 (2004). *Structural Design Actions, Part 5: Earthquake Actions – New Zealand.* Standards New Zealand (NZS) Technical Committee BD-006-04-11, Wellington, New Zealand.

NZSEE (2006). *Assessment and Improvement of the Structural Performance of Buildings in Earthquakes, Recommendations of a NZSEE Study Group on Earthquake Risk of Buildings.* Incorp. corrigenda nos. 1 & 2. New Zealand Society for Earthquake Engineering, Wellington, New Zealand.

Shelton, R.H. (2004). *Seismic Response of Buildings Parts and Non-Structural Components.* Study report, no. 124. BRANZ, Porirua City 5381, New Zealand, ISSN: 0113-3675.

Tasligedik, A.; Pampanin, S.; and Palermo, A. (2011). *Damage Mitigation Strategies of 'Non-Structural' Infill Walls: Concept and Numerical-Experimental Validation Program.* Proc. of the Ninth Pacific Conference on Earthquake Engineering, Building an Earthquake-Resilient Society, Paper Number 120, Auckland, New Zealand, 14-16 April.

Think Brink Australia (2013). *Manual 4: Design of Clay Masonry for Wind and Earthquake.* Artarmon, NSW, Australia. http://www.thinkbrick.com.au/technical-manuals-4?start=0#maincontent

Vaculik, J. (2012). *Unreinforced Masonry Walls Subjected to Out-of-Plane Seismic Actions.* Doctoral Thesis, University of Adelaide, Australia.

Valek, J. and Veiga, R. (2005). *Characterisation of Mechanical Properties of Historic Mortars - Testing of Irregular Samples, Structural Studies, Repairs and Maintenance of Heritage Architecture.* Ninth international conference on structural studies, repairs and maintenance of heritage architecture, Malta, 22-24 June.

Walsh, K.; Dizhur, D.; Almesfer, N.; Cummuskey, P.; Cousins, J.; Derakhshan, H.; Griffith, M.; and Ingham, J. (2014a). *Geometric Characterisation and Out-of-Plane Seismic Stability of Low-Rise Unreinforced Brick Masonry Buildings in Auckland, New Zealand.* Bulletin of the New Zealand Society for Earthquake Engineering, 47(2).

Walsh, K.; Cummuskey, P.; Dizhur, D.; and Ingham, J. (2014b). *Structural Seismic Attributes of Auckland's Commercial Building Stock.* Proc. of the New Zealand Society for Earthquake Engineering Conference, Auckland, New Zealand, 21 – 23 March.